1　**Supplementary Figures 1-10**

2　**Supplementary Figure 1** Maize image analysis and traits extraction.

3　**Supplementary Figure 2** Distribution of QTL mapping resolution.

4　**Supplementary Figure 3** Correlation coefficients between paired traits for 42 traits investigated at 16 time points.

5　**Supplementary Figure 4** Chromosomal distribution of identified QTLs with 42 primary phenotypic traits and 64 growth related traits.

6　**Supplementary Figure 5** Comparison of heat maps for QTLs density between metabolic and investigated phenotypic traits in By804/B73

7　recombination population.

8　**Supplementary Figure 6** Predication ability comparison of 6 models for digital biomass accumulation.

9　**Supplementary Figure 7** The RNA-seq gene atlas for four genes (GRMZM2G180490, GRMZM2G010702, GRMZM2G151649 and

10　GRMZM2G057023).

11　**Supplementary Figure 8** Experimental design.

12　**Supplementary Figure 9** The image analysis interface designed in the study.

13　**Supplementary Figure 10** The flow chart of the program. The number represents the processing module of the following figure 1~10.
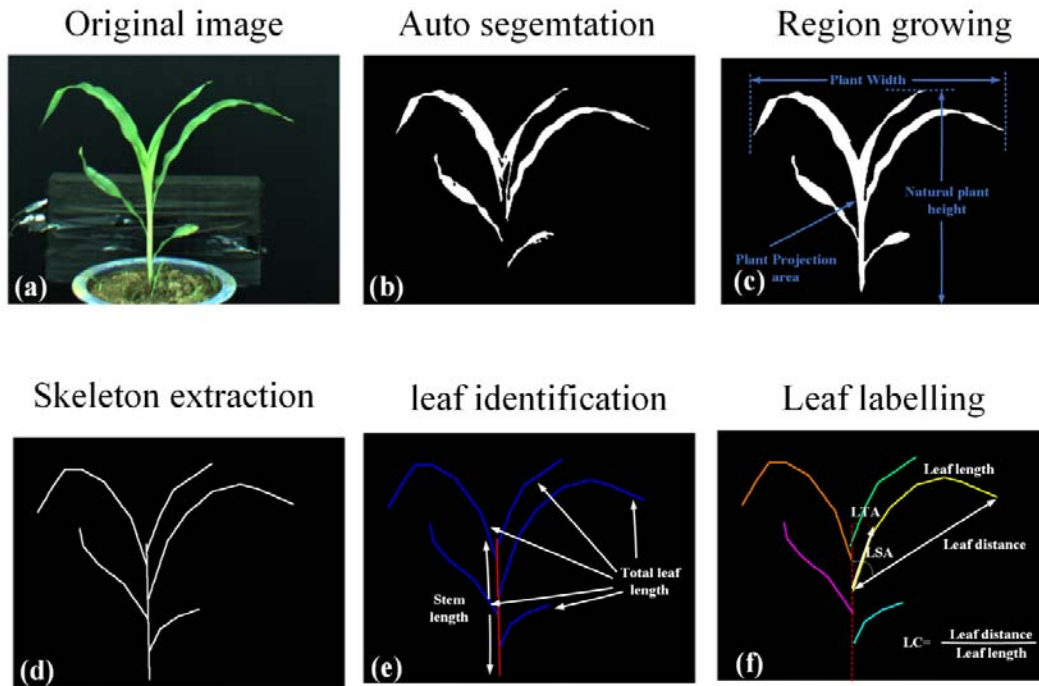
14

15　**Supplementary Tables 1-12**

16　**Supplementary Table 1** The 106 traits classification and abbreviation.

17　**Supplementary Table 2** Statistical summary of the 10 developed models for fresh weight estimation (sample size = 387).

Supplementary Figure 1 Maize image analysis and traits extraction. (a) The side-view image with maximum area was selected in 15 side-view images; (b) ExG component was extracted and the OTSU method was applied to obtain the binary image; (c) Specified region growing algorithm was developed to acquire the whole plant image, then plant morphological traits, color traits, biomass related traits, and histogram traits were extracted; (d) The parallel thinning algorithm was used to extract the skeleton image; (e) The Hough transformation was applied to recognize the stem skeleton; (f) Each leaf branch was identified, meanwhile, leaf architecture traits were calculated during the image analysis process. With biomass (fresh weights and dry weights) at different time points were obtained, growth related traits were calculated.

Mapping Resolation (1LOD)
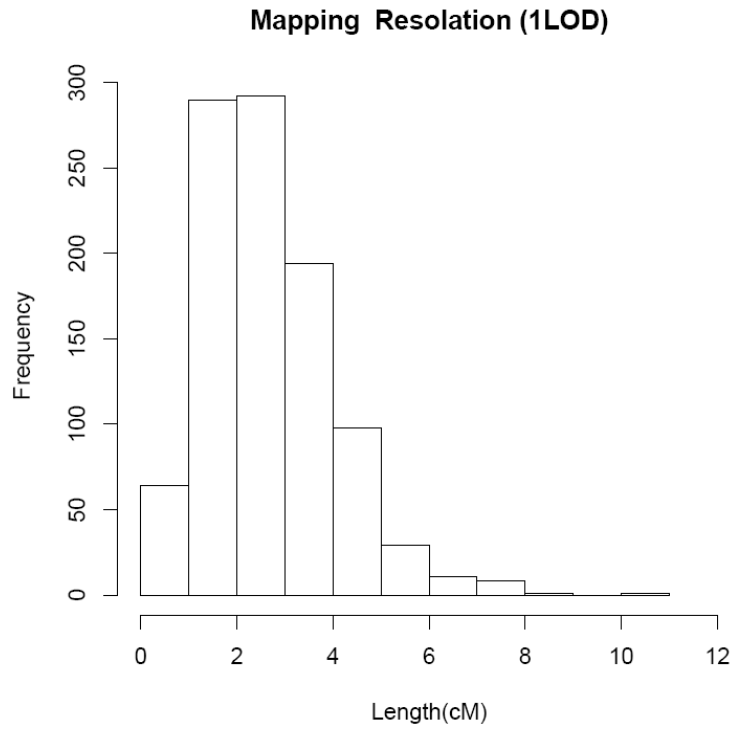
45
46

47 **Supplementary Figure 2 Distribution of QTL mapping resolution.**

48 Confidence interval for each QTL was assigned as one-LOD drop of the peak which

49 was regarded as mapping resolution.

50
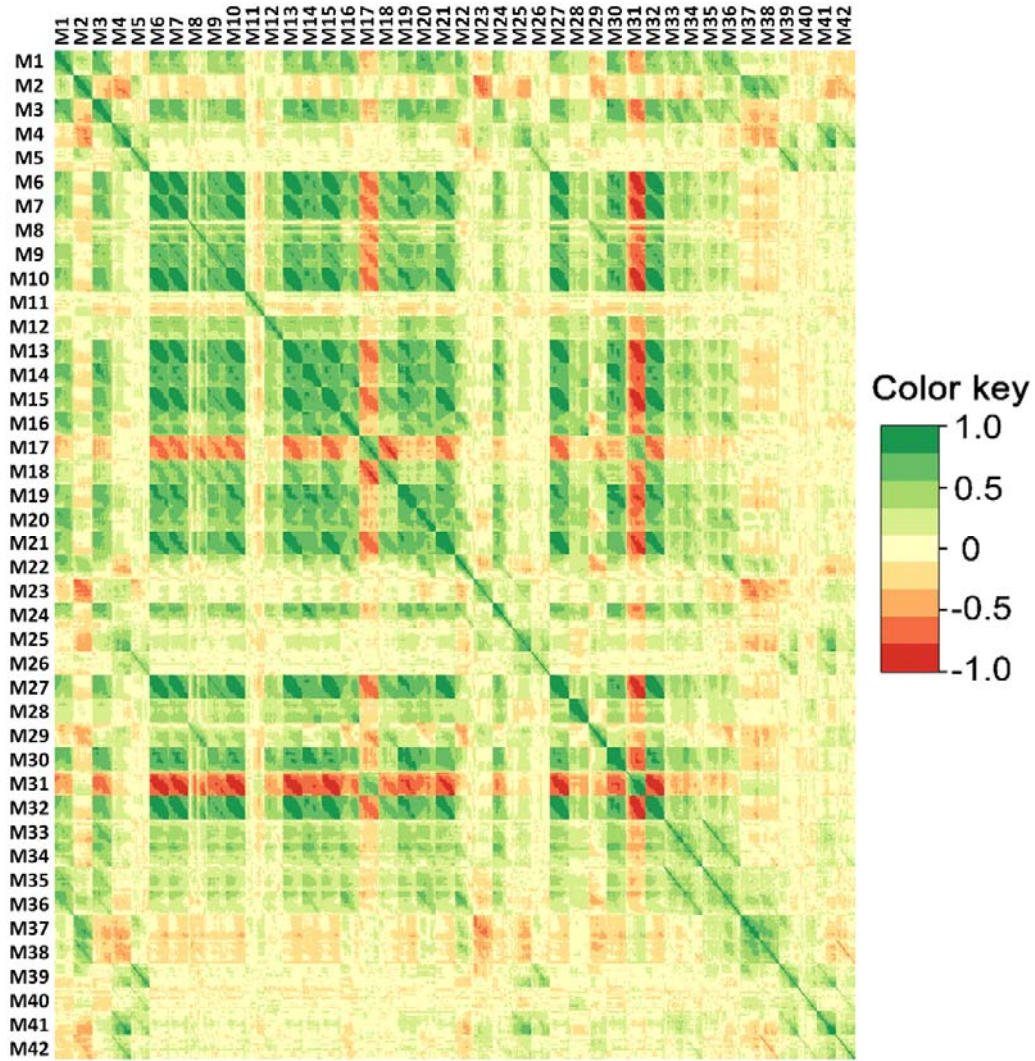
Supplementary Figure 3 Correlation coefficients between paired traits for 42 traits investigated at 16 time points. The x axis from left to right and y axis from top to bottom indicate time points (e.g. from T1 to T16) for each of 42 traits. M1, LNL; M2, LC; M3, SLL; M4, LSA; M5, LTA; M6, DW; M7, E_TEX; M8, FDIC; M9, FDNIC; M10, FW; M11, GCV; M12, LN; M13, M_TEX; M14, MPH; M15, MU3_TEX; M16, NPH; M17, PAR; M18, PC; M19, PP; M20, PW; M21, S_TEX; M22, SDLNL; M23, SDLC; M24, SDSLL; M25, SDLSA; M26, SDLTA; M27, SE_TEX; M28, SL; M29, TBR; M30, TLL; M31, U_TEX; M32, SA; M33, SLL_below; M34, SLL_above; M35, LNL_below; M36, LNL_above; M37, LC_below; M38, LC_above; M39, LTA_below; M40, LTA_above; M41, LSA_below; M42, LSA_above.
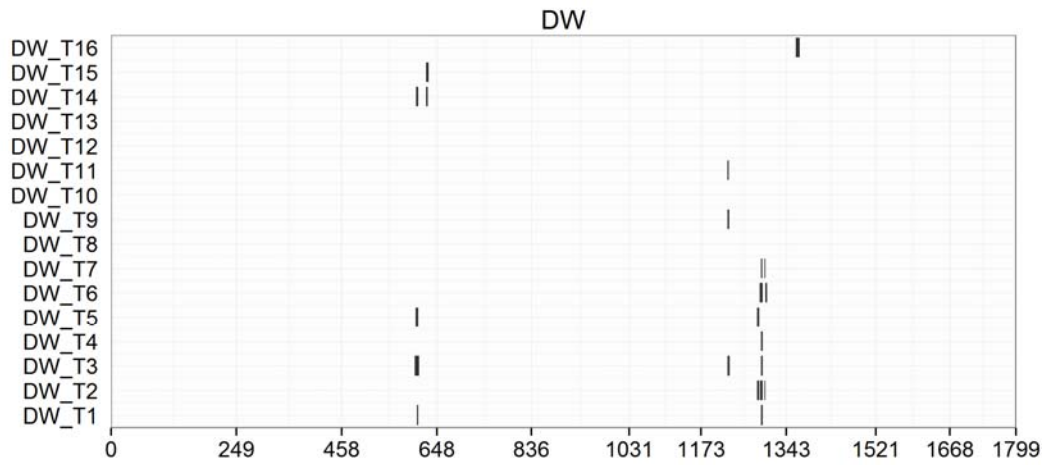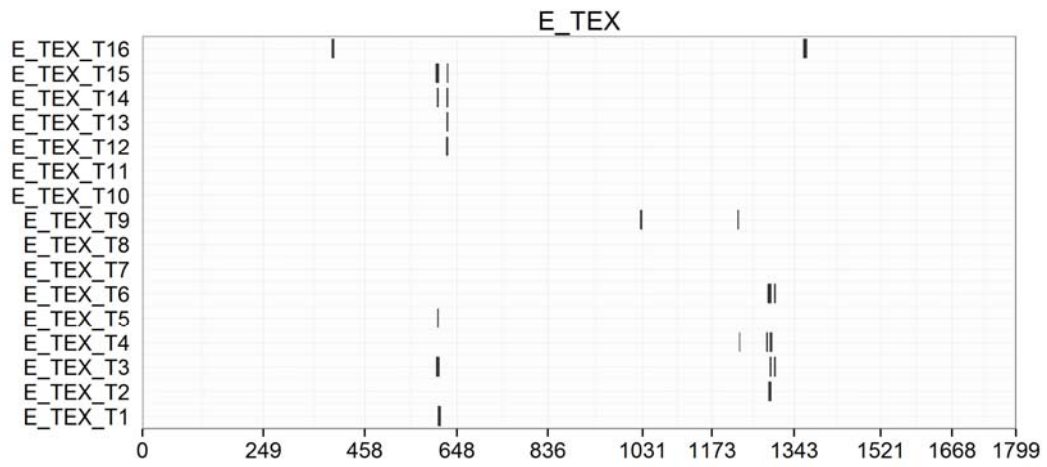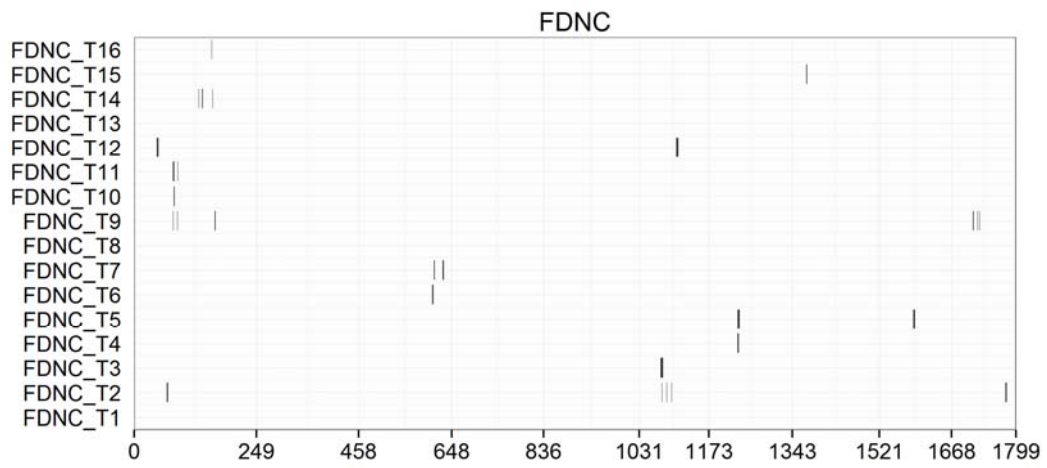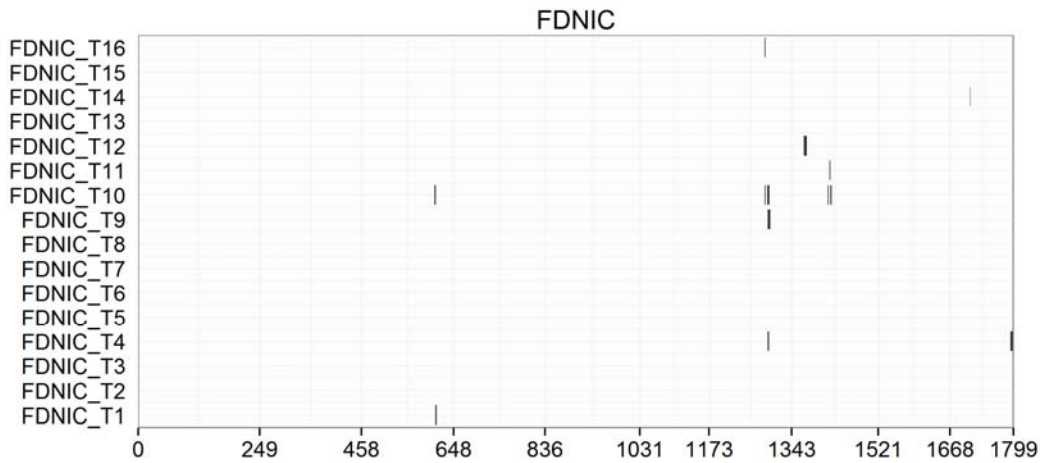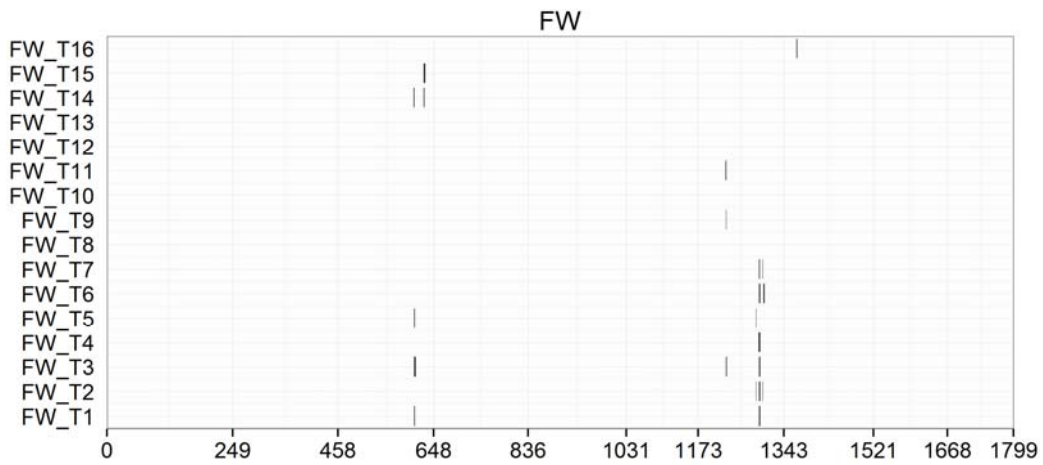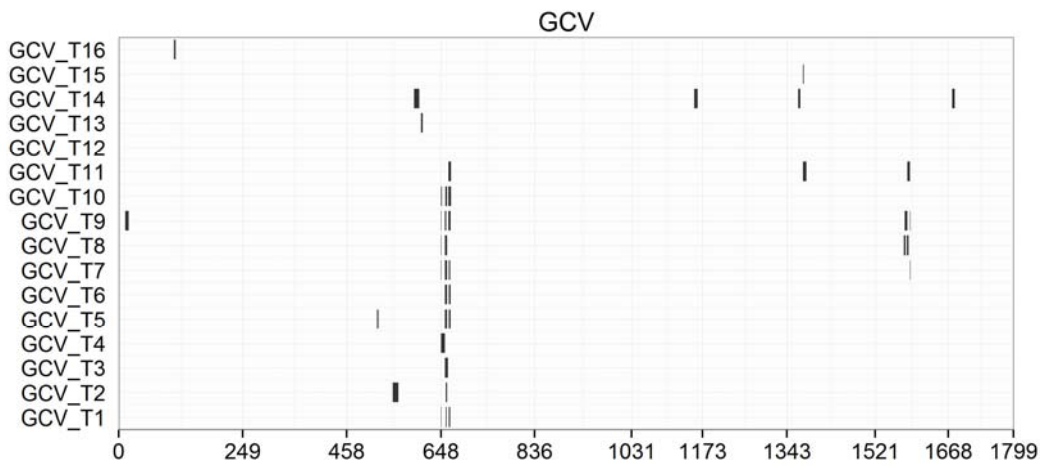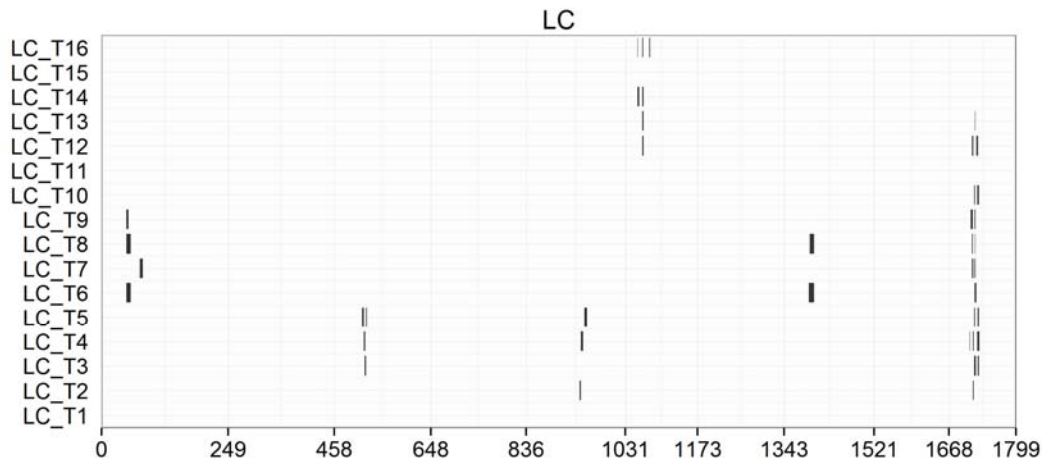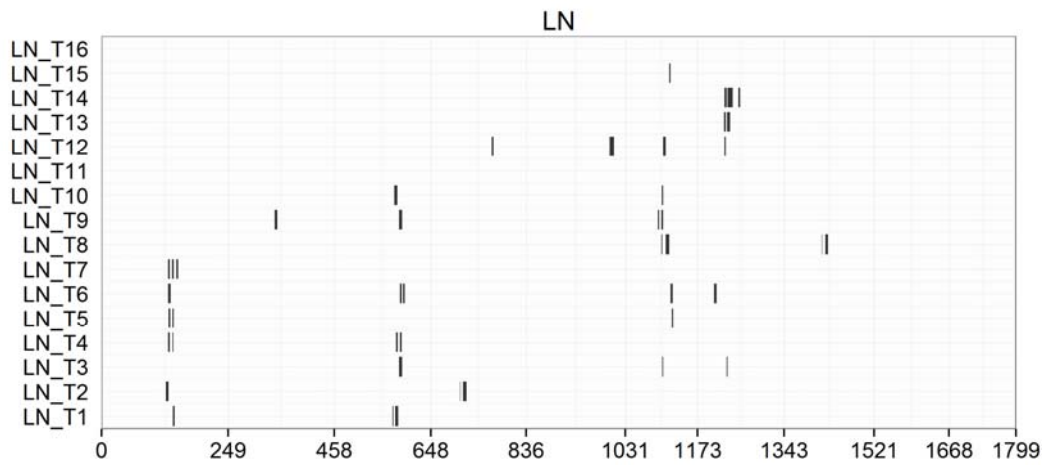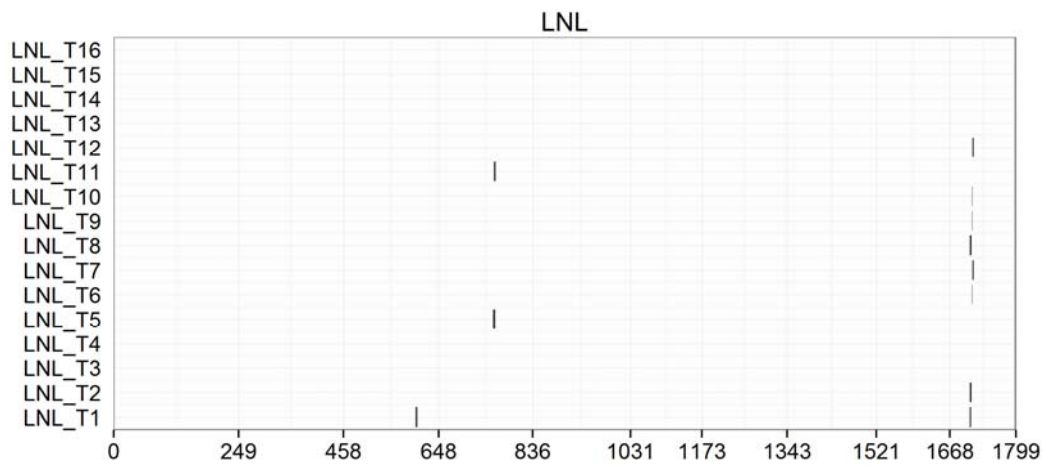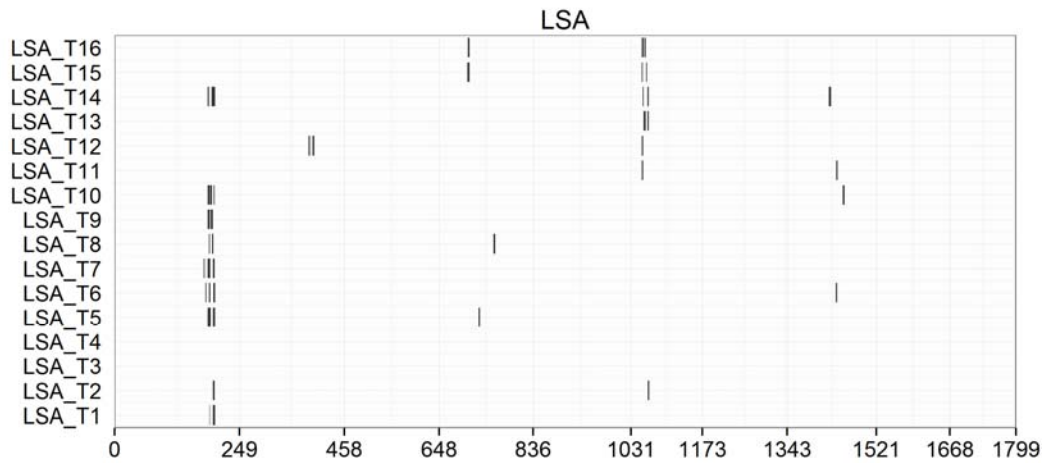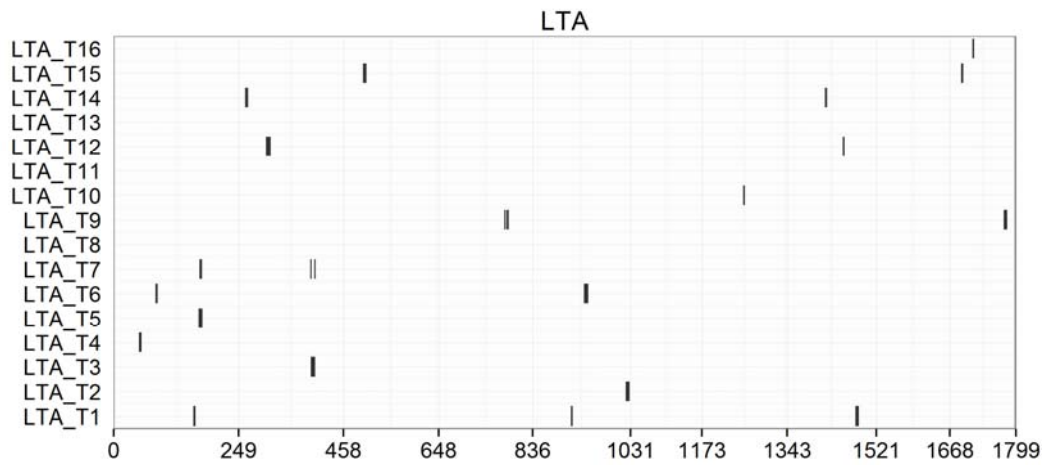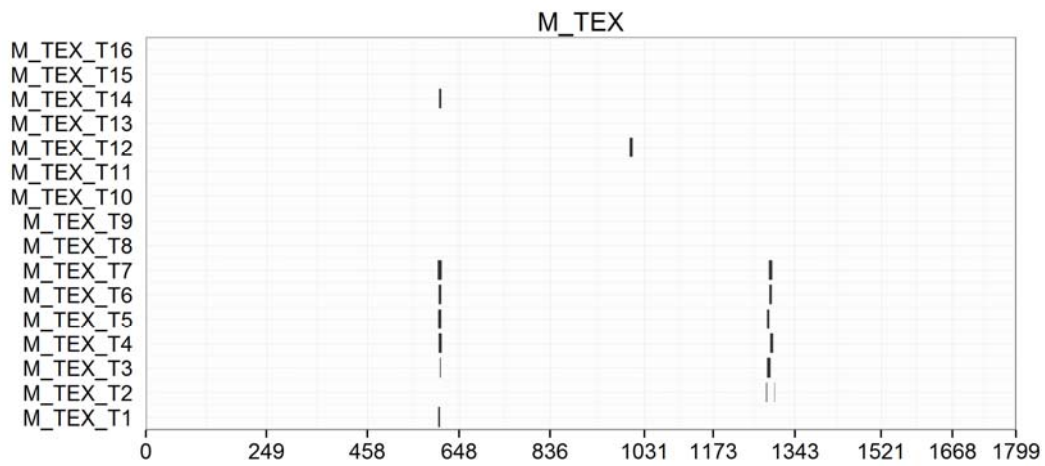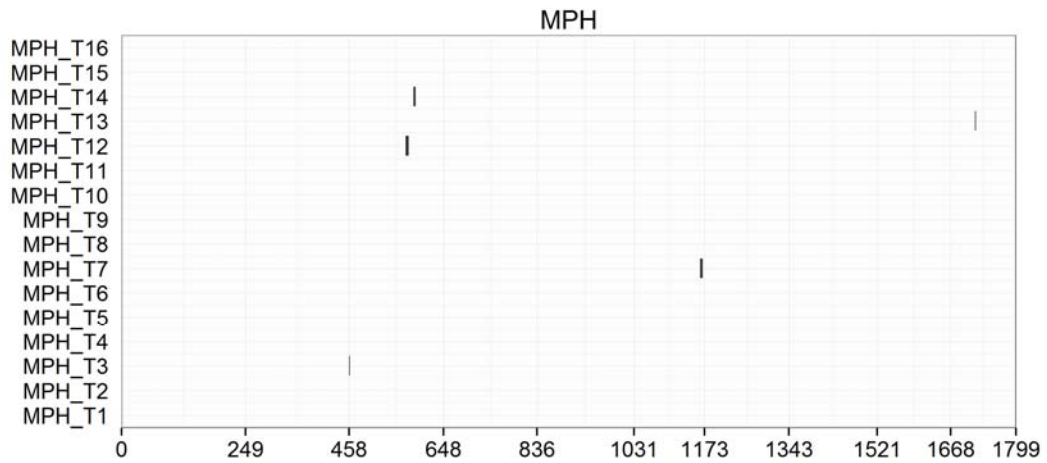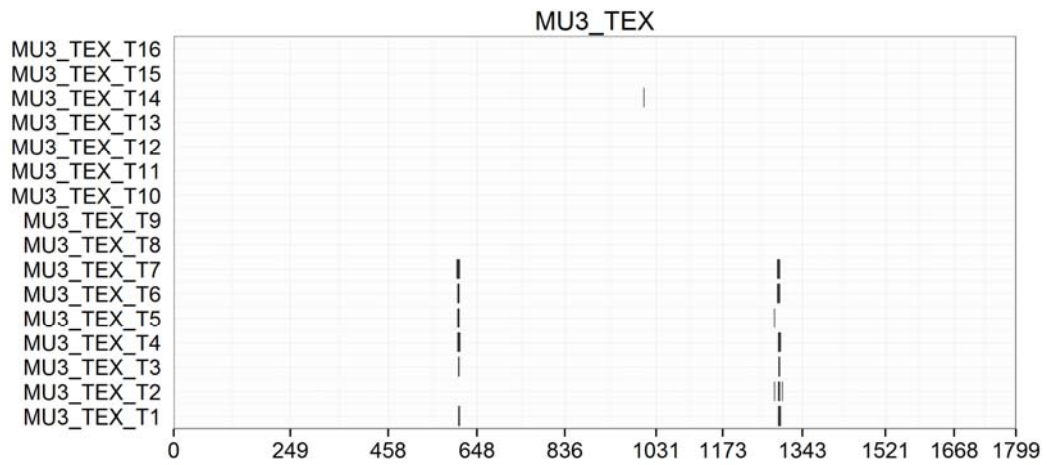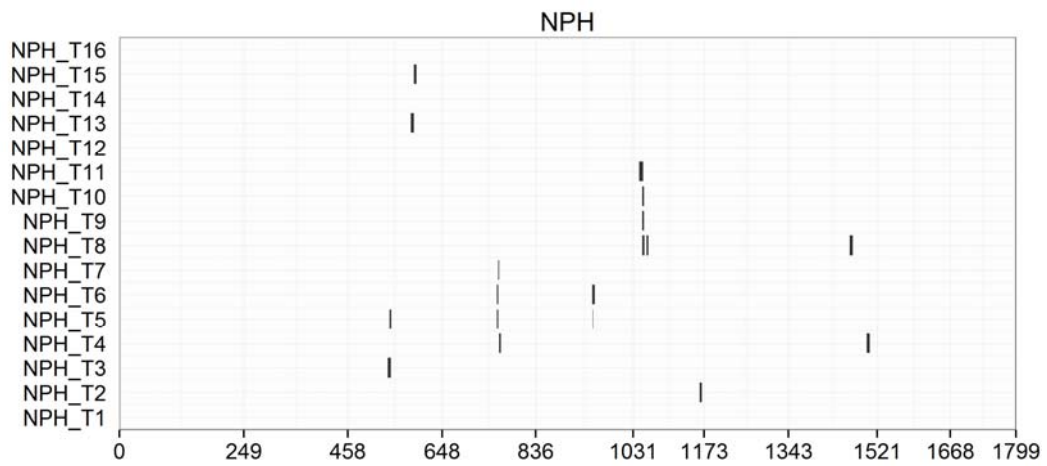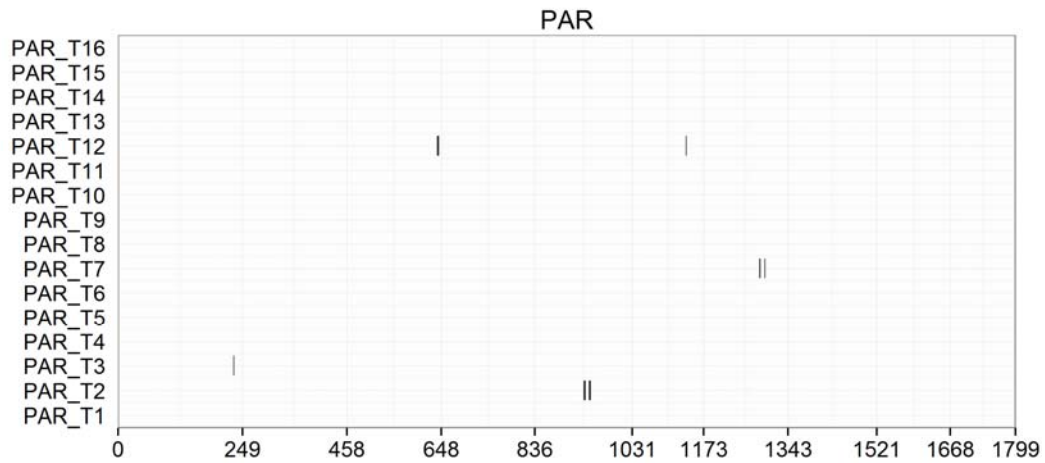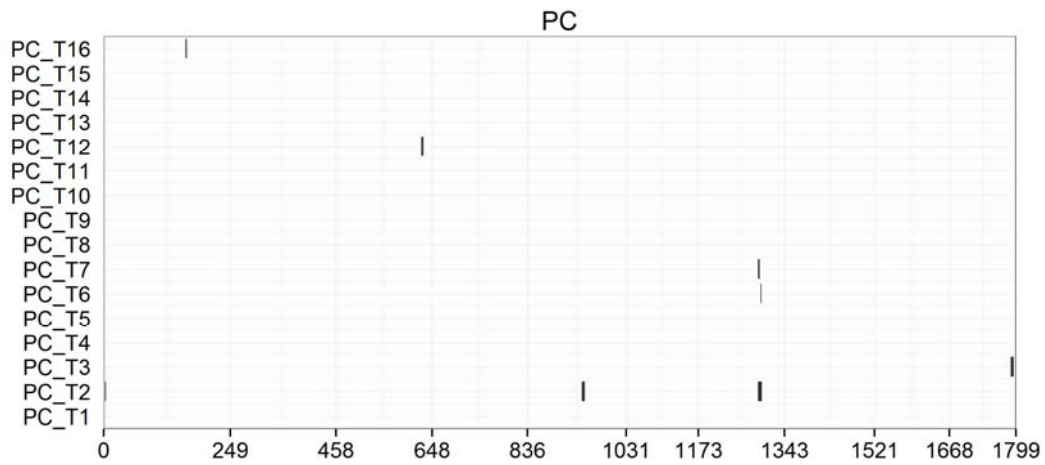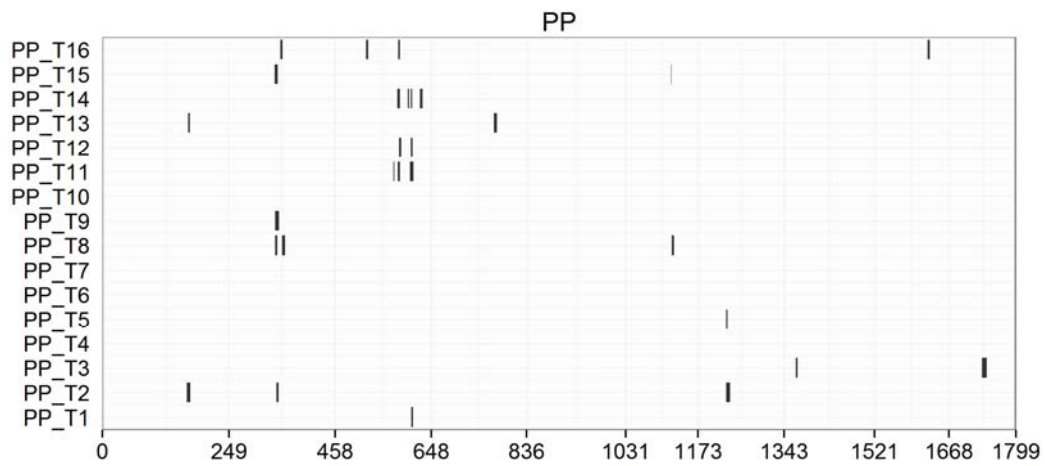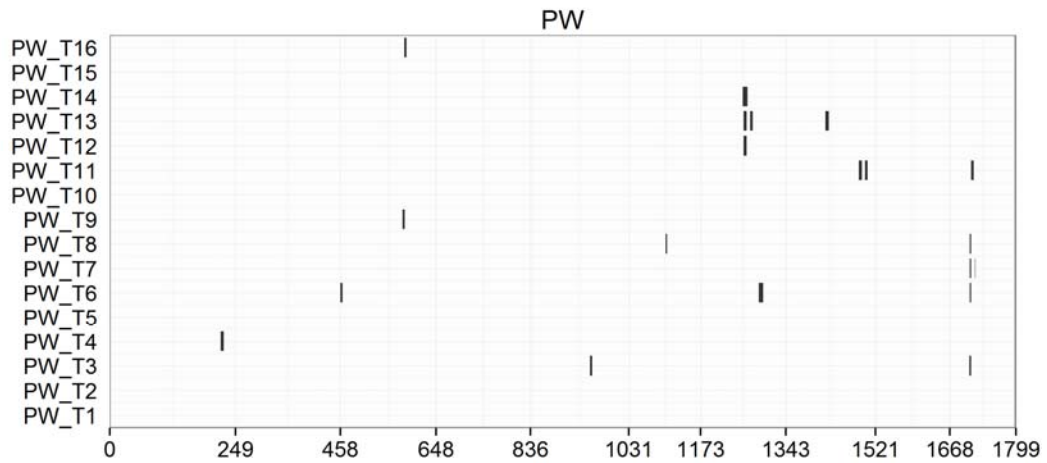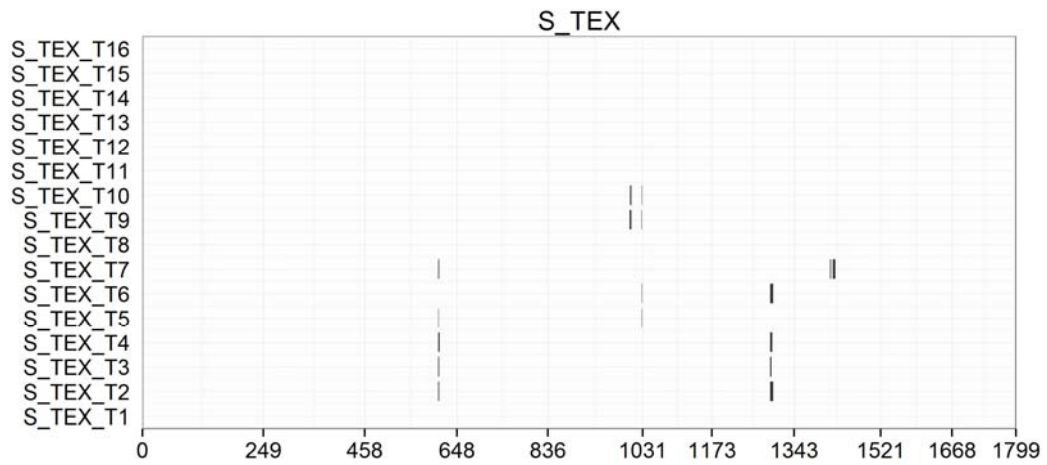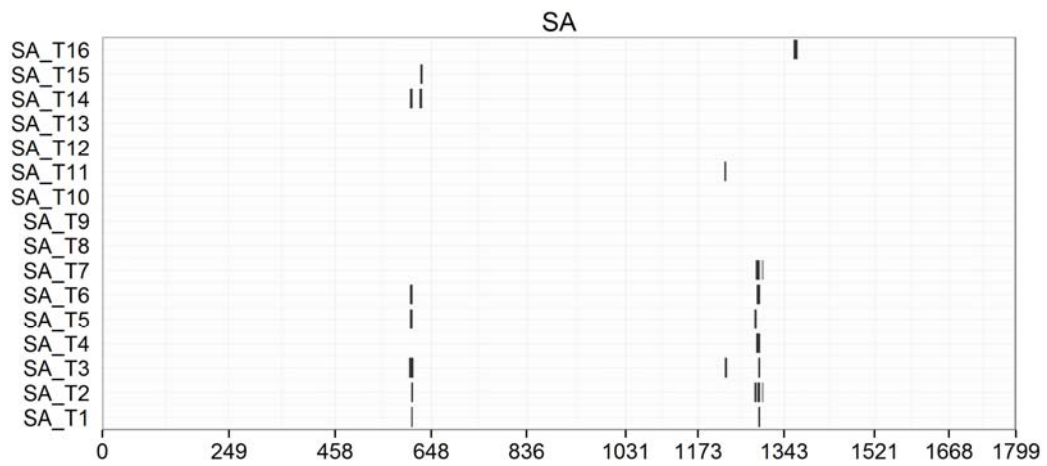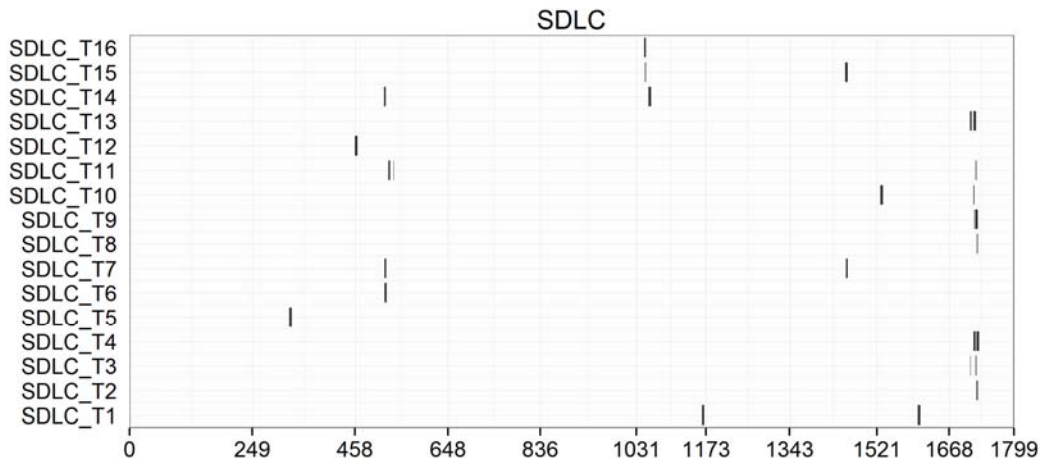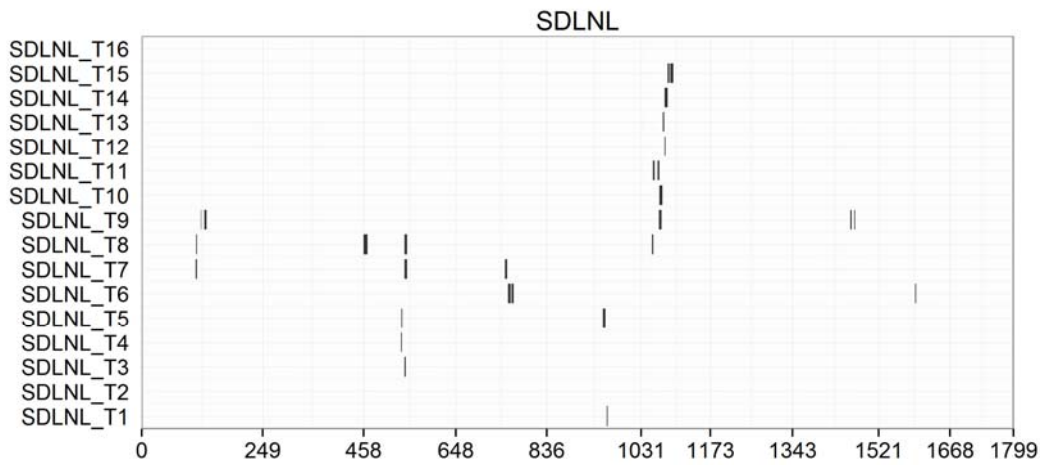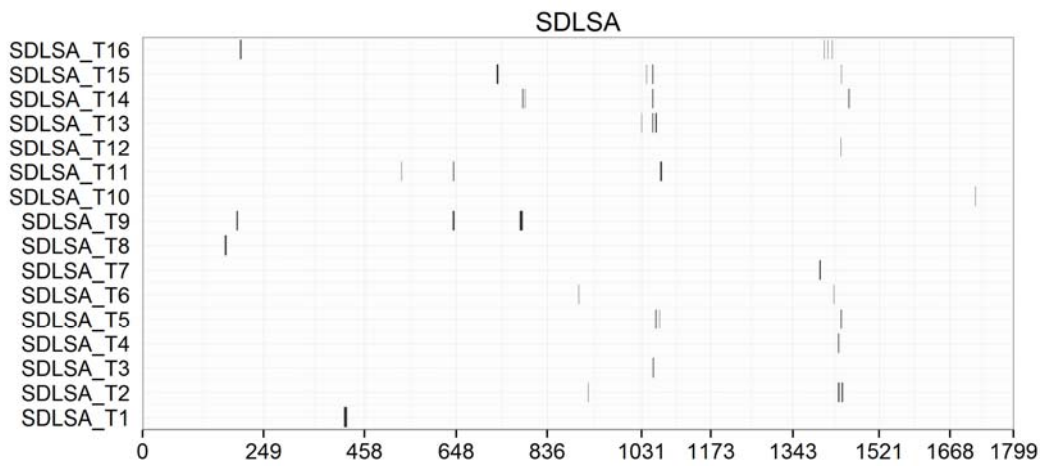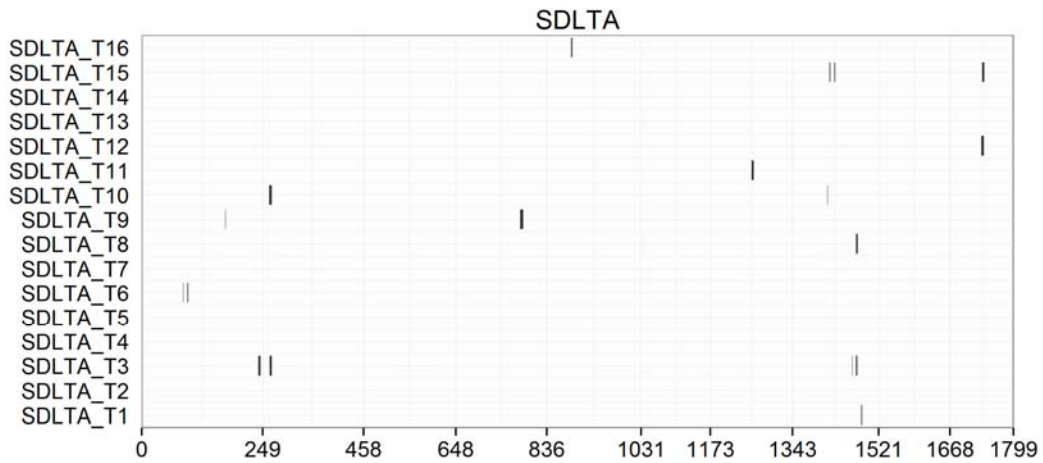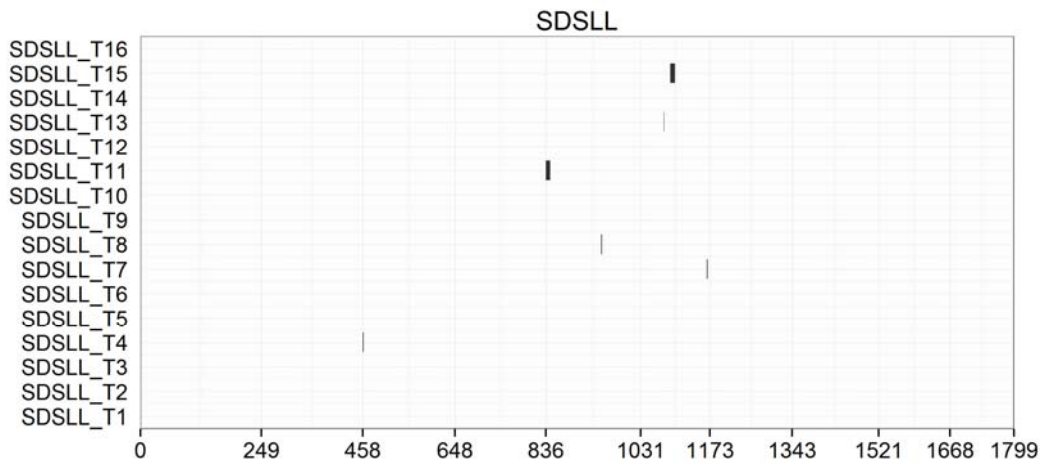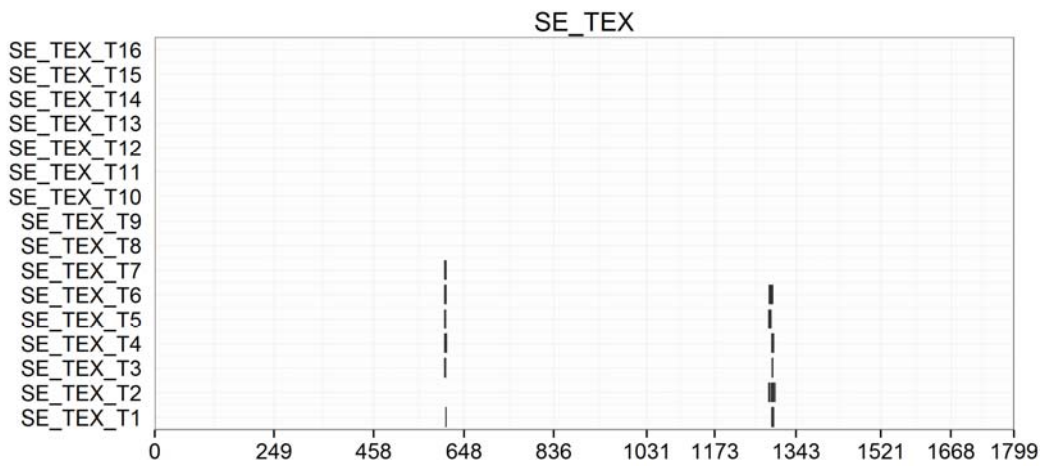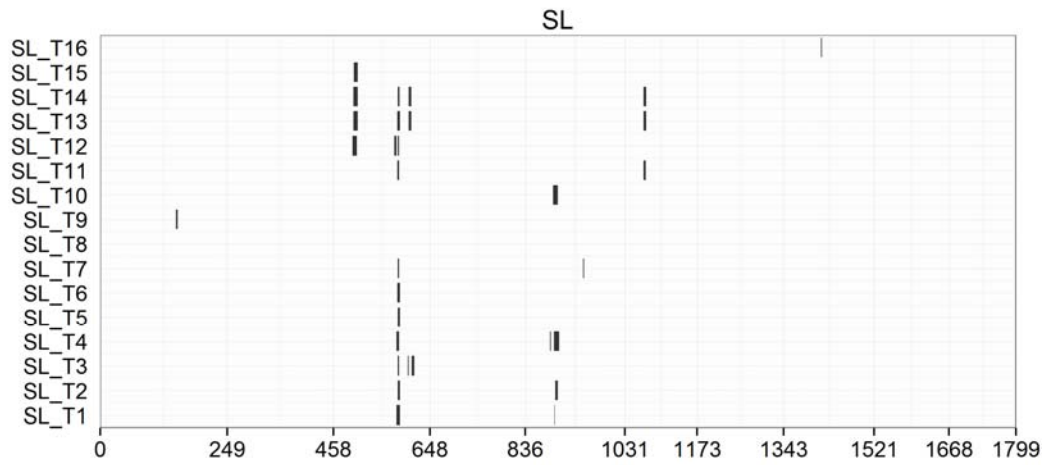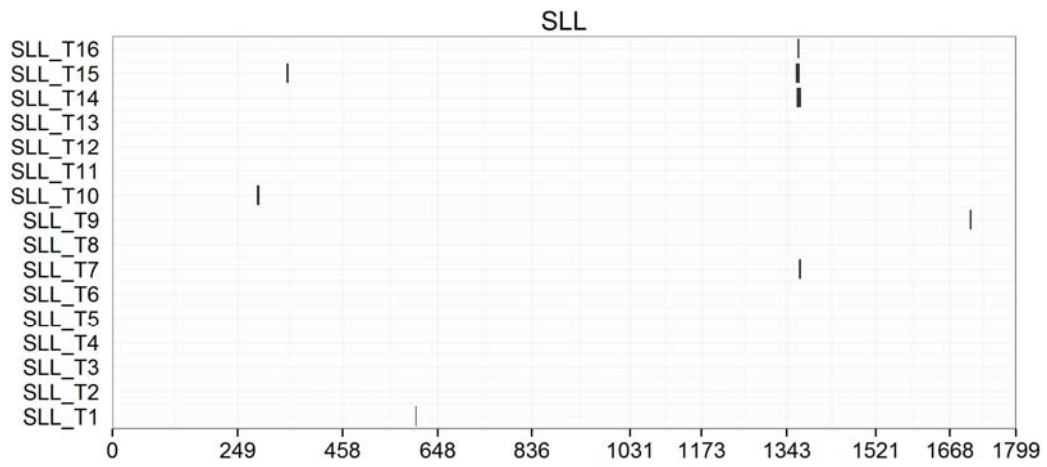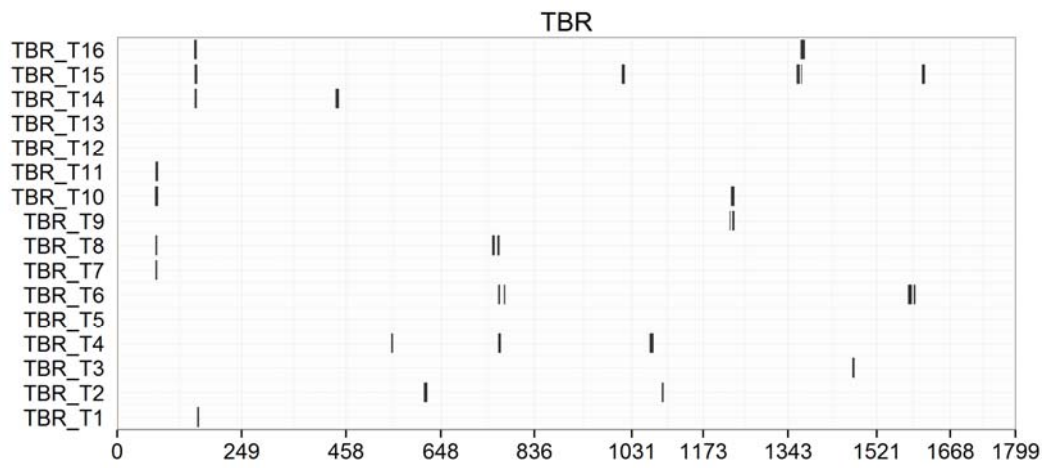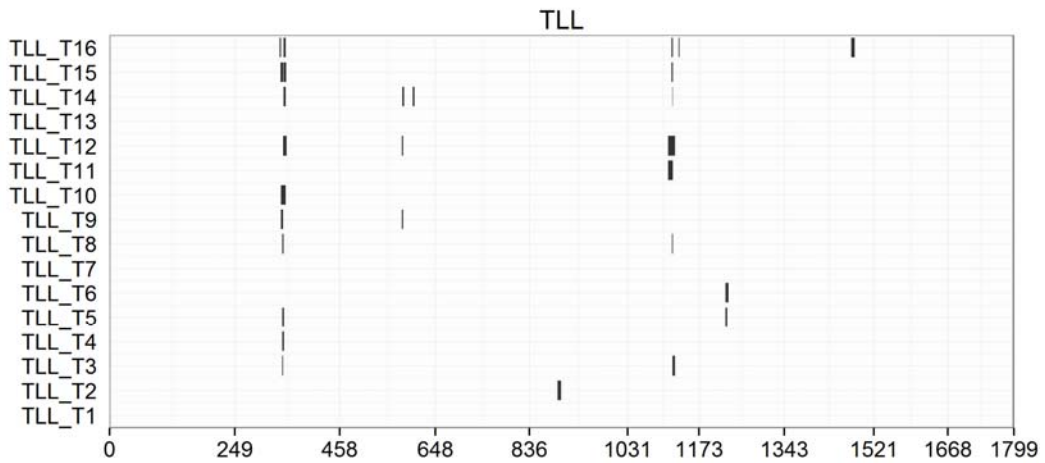
DW

63

E_TEX

64

FDNC

65

66

67

68

LC

69

LN

70

LNL

71

72

73

74

MPH

75

MU3_TEX

76

NPH

77

PAR

78

PC

79

PP

80

PW

81

S_TEX

82

SA

83

SDLC

84

SDLNL

85

SDLSA

86

SDLTA

87

SDSLL

88

SE_TEX

89

14

SL

90

SLL

91

TBR

92

TLL

93

LC_above

94

LC_below

95

LNL_above

96

LNL_below

97

LSA_above

98

17

LSA_below

99

LTA_above

100

LTA_below

101

18

SLL_above

102

AGR_DW

103

AGR_FW

104

105

106
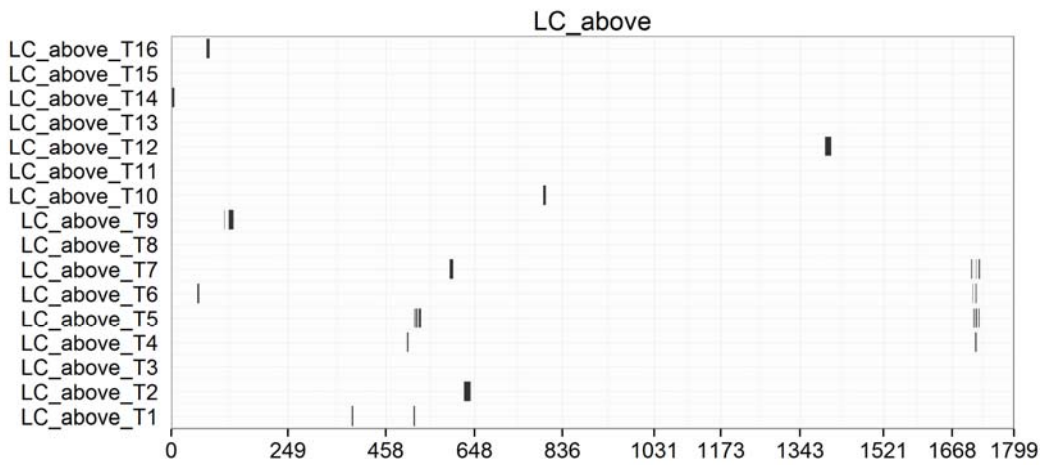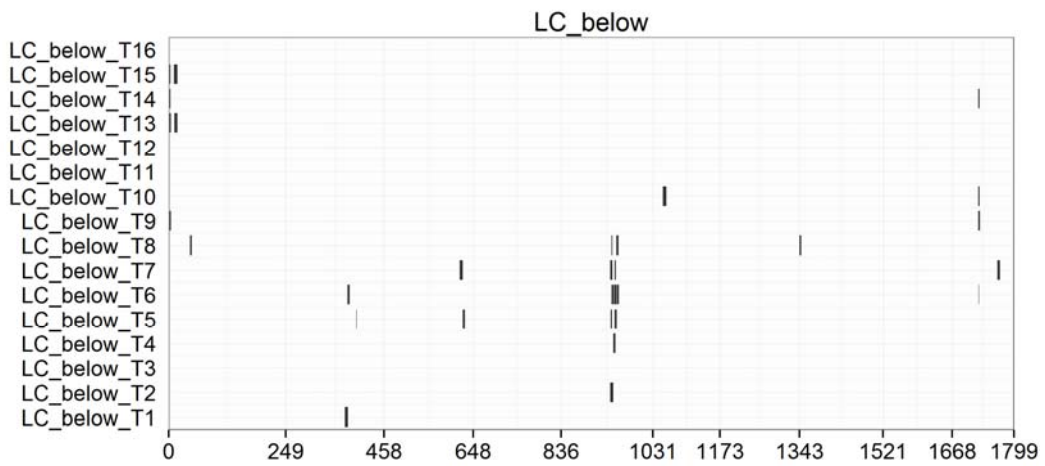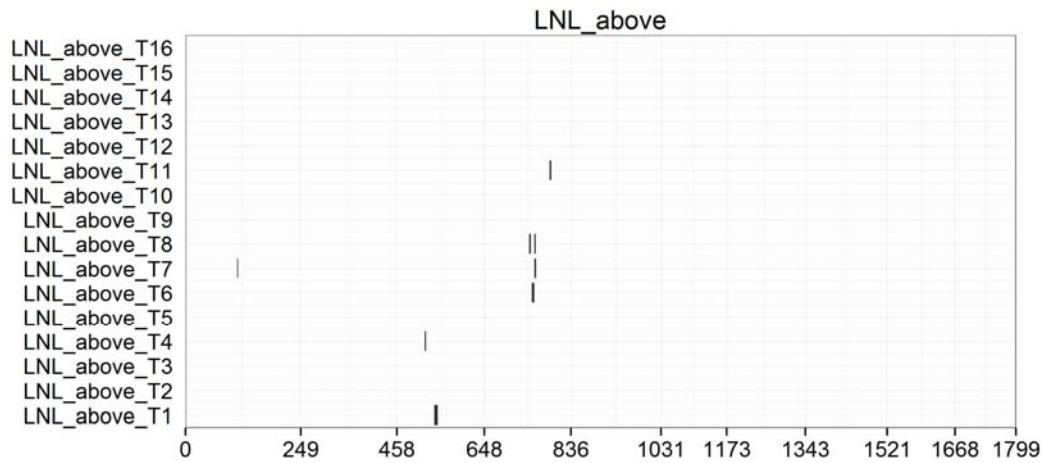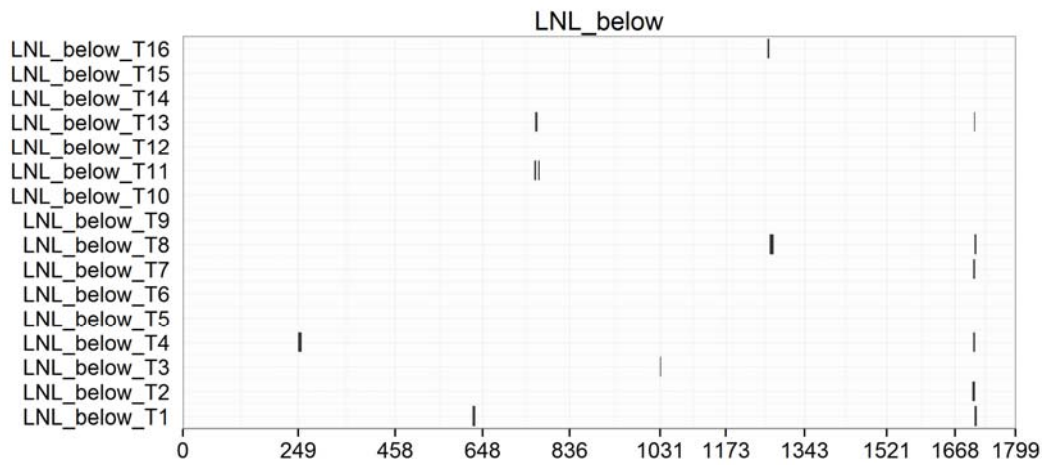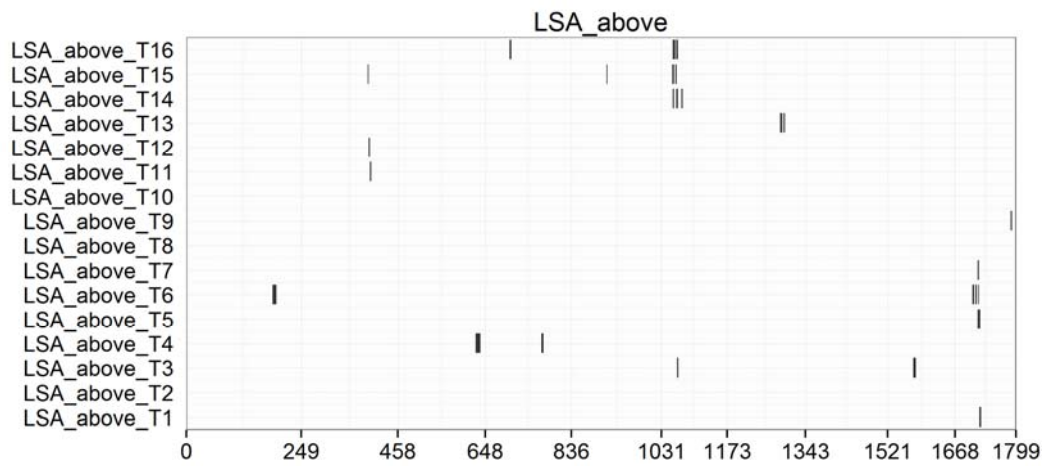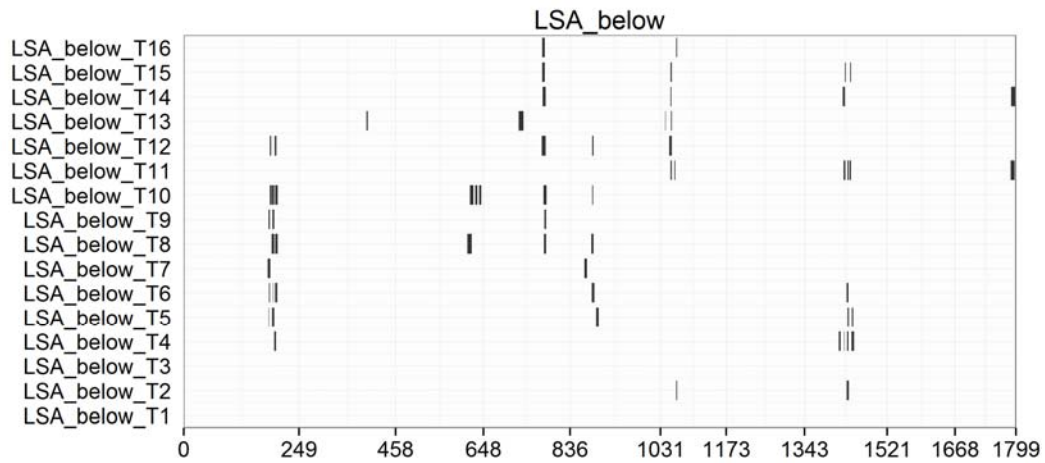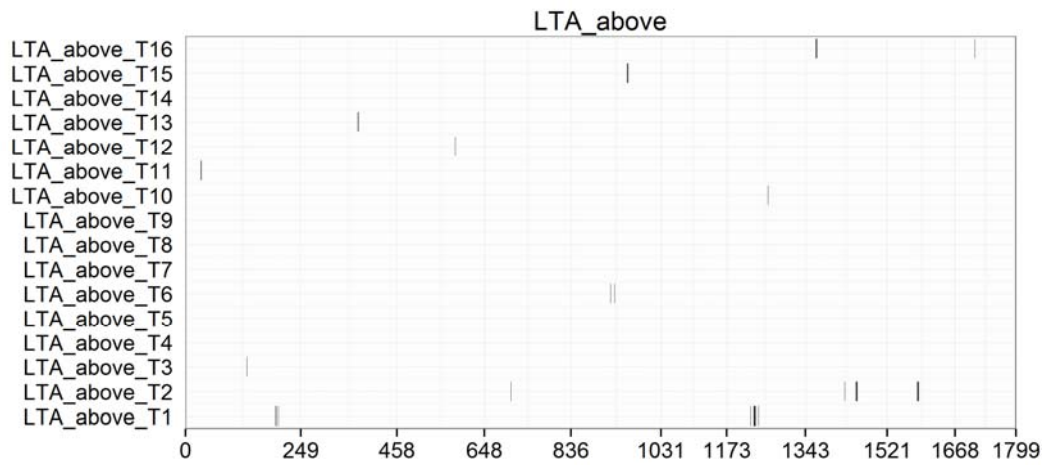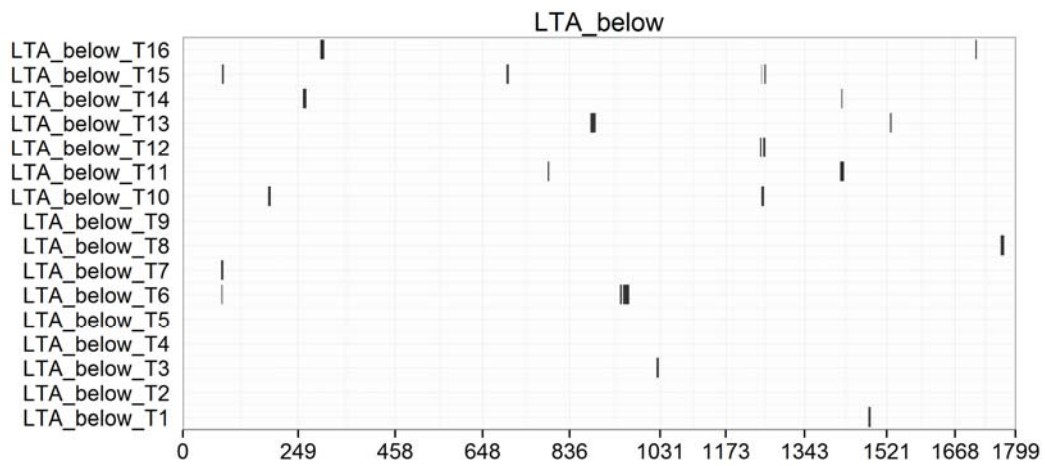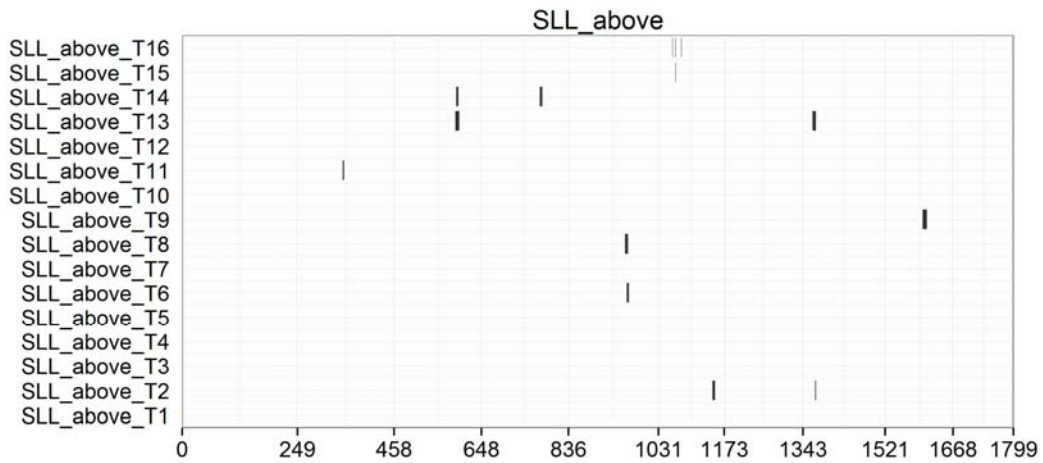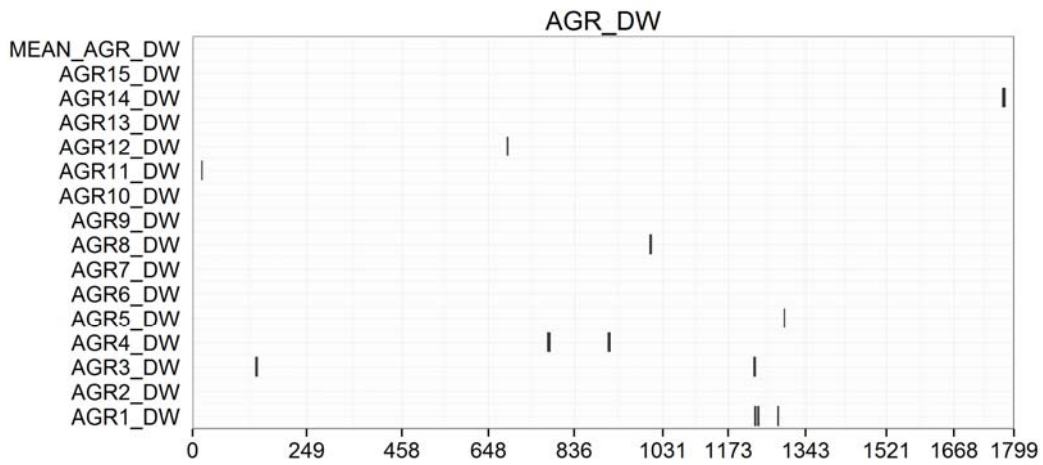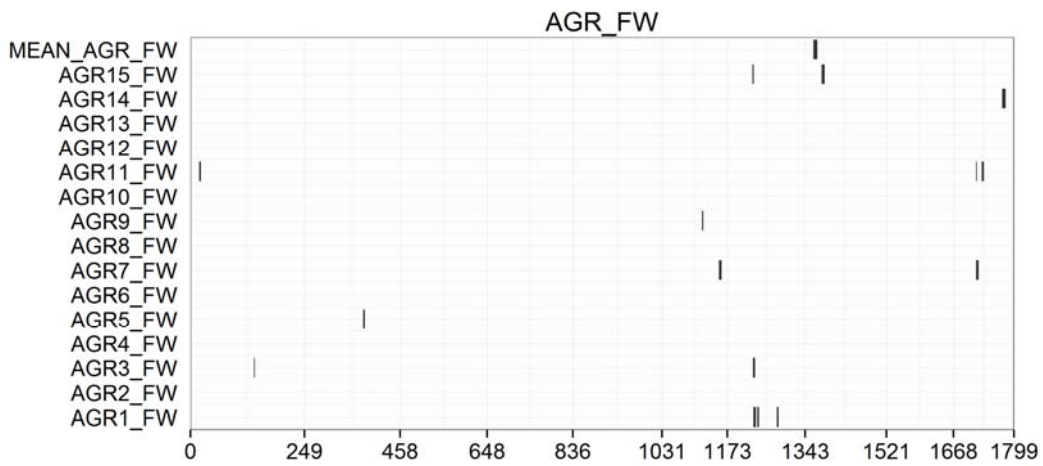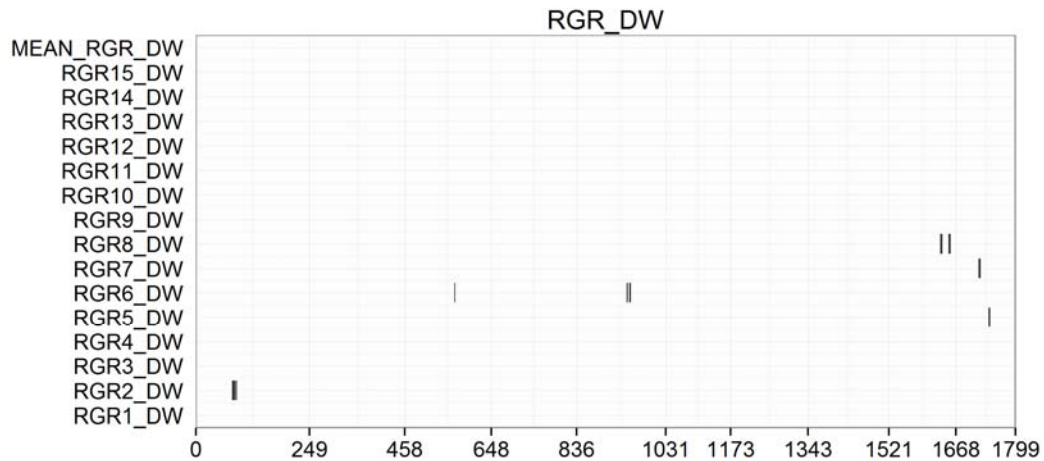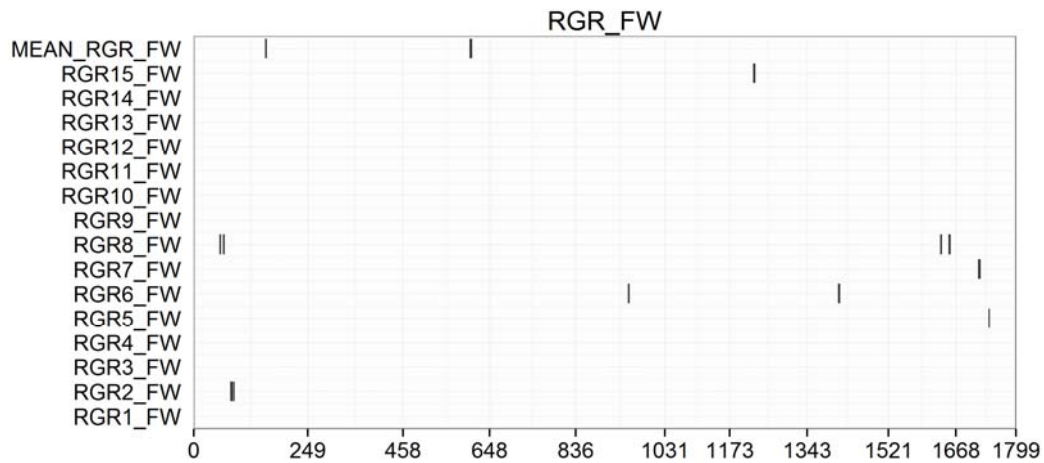
Supplementary Figure 4 Chromosomal distribution of identified QTLs with 42 primary phenotypic traits and 64 growth related traits. QTL regions (represented by the confidence interval for each QTL was assigned as 1-LOD drop of the peak) across the maize genome responsible for investigated phenotypic traits, growth rate related traits are shown as black solid rectangular boxes. The x axis indicates the genetic positions across the maize genome in cM. Detailed information of all detected QTLs is shown in Supplemental Data 2.

114
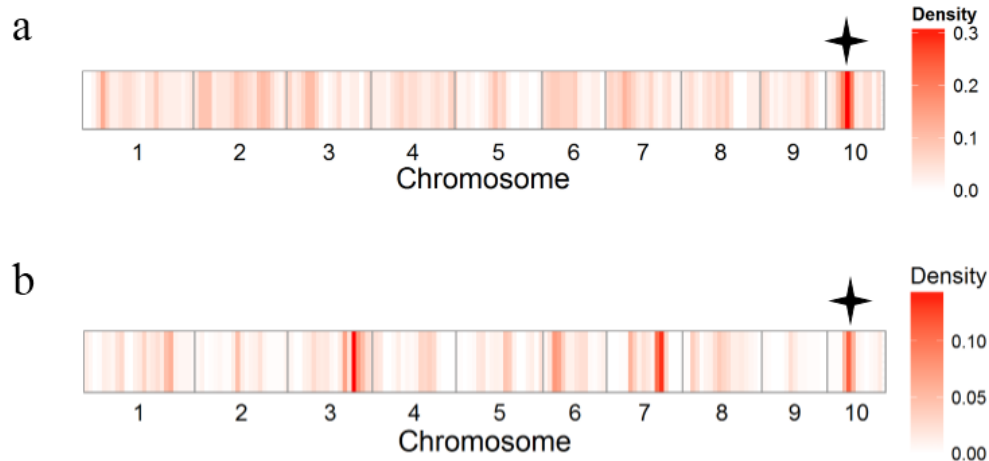
Supplementary Figure 5 Comparison of heat maps for QTLs density between metabolic and investigated phenotypic traits in By804/B73 recombination population. (a) Heat map of density of metabolic QTL across the genome. (b) Heat map of density of investigated phenotypic traits QTL across the genome. The black asterisk indicates the QTL hot regions on chromosome 10 were both detected in metabolic and investigated phenotypic traits.

Training set

Testing set

Linear model

Power model

Exponential model

logarithm model

Quadratic polynomial model

Logistic model

122

22
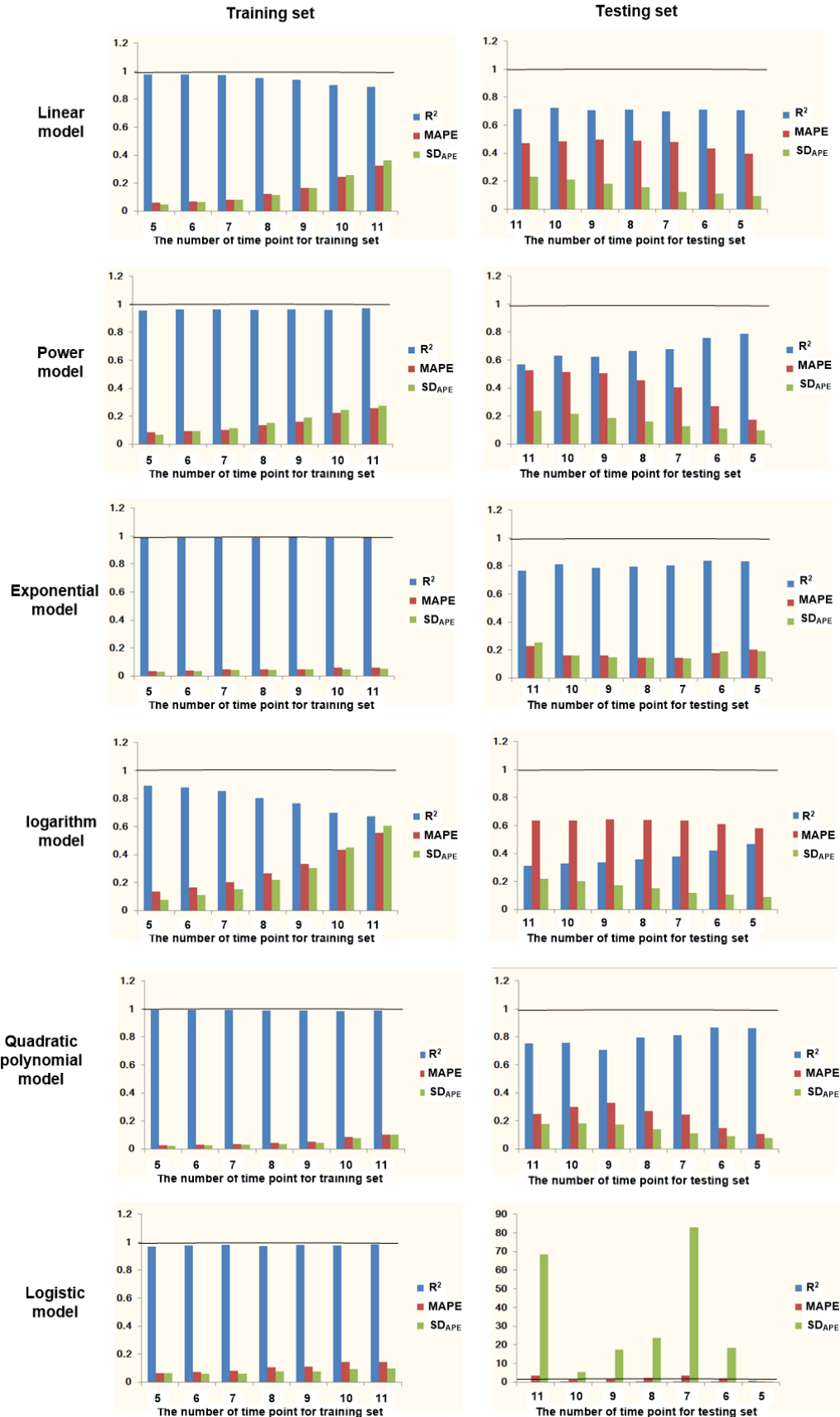
123 **Supplementary Figure 6 Predication ability comparison of 6 models for digital**

124 **biomass accumulation.** The left part indicated the fit quality of 6 models with

125 training set (including the linear, power, exponential, logarithm, quadratic

126 polynomial, and logistic model). The right part indicated the fit quality of 6 models

127 with the corresponding testing set. The total number of time points for modeling was

128 16, thus if the number of time point for training set was 5 (time points 1-5), the

129 corresponding number of time point for testing set was 11 (time points 6-16), which

130 were shown in the x-coordinate in the images. The average R^2, MAPE, and SD_{APE}

131 value were indicated. Both in the training set and testing set, the exponential model

132 presented the best fitted model, which indicated compared with other 5 models, the

133 exponential model had better predication ability for digital biomass accumulation

134 during the seedling stage to tasseling stage. The black line indicated the value 1.

135

GRMZM2G180490

GRMZM2G180490

FPKM 108.9 ... 108.9 FPKM

1. Primary_Root_3DAS (0)
2. Root_MZ_and_EZ_3DAS (0)
3. Root_DZ_3DAS (0)
4. Root_CP_3DAS (0)
5. Root_Stele_3DAS (0)
6. Primary_Root_GH_6DAS (0)
7. Root_System_7DAS (0)
8. Primary_Root_7DAS (0.3)
9. Seminal_Roots_7DAS (0)
10. Primary_Root_Z1_7DAS (0)

11. Primary_Root_Z2_7DAS (0)
12. Primary_Root_Z3_7DAS (0)
13. Primary_Root_Z4_7DAS (0)
14. Crown_Roots_Nodes1-3_V7 (0)
15. Crown_Roots_Node4_V7 (0)
16. Crown_Roots_Node5_V7 (1.6)
17. Crown_Roots_Node5_V13 (0.9)
18. Brace_Roots_Node6_V13 (0)
19. Coleoptile_GH_6DAS (15.6)
20. Pooled_Leaves_V1 (0)

21. Topmost_Leaf_V3 (5.3)
22. Shoot_Tip_V5 (6.0)
23. Tip_Stage2_Leaf_V5 (0)
24. Base_Stage2_Leaf_V5 (49.7)
25. Tip_Stage2_Leaf_V7 (0)
26. Base_Stage2_Leaf_V7 (64.9)
27. Eighth_Leaf_V9 (0)
28. Eleventh_Leaf_V9 (0)
29. Thirteenth_Leaf_V9 (17.6)
30. Immature_Leaves_V9 (46.8)

31. Thirteenth_Leaf_VT (0)
32. Thirteenth_Leaf_R2 (0)
33. Leaf_0DAP (0)
34. Leaf_6DAP (0)
35. Leaf_12DAP (0)
36. Leaf_18DAP (0)
37. Leaf_24DAP (0)
38. Leaf_30DAP (0)
39. Stem_and_SAM_V1 (37.2)
40. Stem_and_SAM_V3 (28.4)

41. First_Internode_V5 (3.1)
42. Fourth_Internode_V9 (0)
43. Internode_0DAP (1.5)
44. Internode_6DAP (0)
45. Internode_12DAP (0)
46. Internode_18DAP (0)
47. Internode_24DAP (0)
48. Internode_30DAP (0)
49. Immature_Tassel_V13 (82.4)
50. Meiotic_Tassel_V18 (19.2)

51. Anthers_R1 (2.6)
52. Immature_Cob_V18 (8.0)
53. Pre-pollination_Cob_R1 (93.2)
54. Silks_R1 (59.7)
55. Whole_Seed_2DAP (99.2)
56. Whole_Seed_4DAP (108.9)
57. Whole_Seed_6DAP (59.8)
58. Whole_Seed_8DAP (60.5)
59. Whole_Seed_10DAP (27.8)
60. Whole_Seed_12DAP (2.2)

61. Whole_Seed_14DAP (0)
62. Whole_Seed_16DAP (5.3)
63. Whole_Seed_18DAP (3.9)
64. Whole_Seed_20DAP (0)
65. Whole_Seed_22DAP (0)
66. Whole_Seed_24DAP (0)
67. Endosperm_12DAP (0)
68. Endosperm_14DAP (0)
69. Endosperm_16DAP (0)
70. Endosperm_18DAP (0)

71. Endosperm_20DAP (0)
72. Endosperm_22DAP (0)
73. Endosperm_24DAP (0)
74. Embryo_16DAP (43.5)
75. Embryo_18DAP (25.1)
76. Embryo_20DAP (18.3)
77. Embryo_22DAP (10.4)
78. Embryo_24DAP (15.8)
79. Pericarp_18DAP (21.0)

137

138

GRMZM2G010702

GRMZM2G010702

FPKM 73.6 ... 73.6 FPKM

1. Primary_Root_3DAS (2.1)
2. Root_MZ_and_EZ_3DAS (0)
3. Root_DZ_3DAS (12.0)
4. Root_CP_3DAS (5.9)
5. Root_Stele_3DAS (6.1)
6. Primary_Root_GH_6DAS (10.7)
7. Root_System_7DAS (13.4)
8. Primary_Root_7DAS (9.2)
9. Seminal_Roots_7DAS (6.2)
10. Primary_Root_Z1_7DAS (0.8)

11. Primary_Root_Z2_7DAS (2.7)
12. Primary_Root_Z3_7DAS (7.4)
13. Primary_Root_Z4_7DAS (73.6)
14. Crown_Roots_Nodes1-3_V7 (2.4)
15. Crown_Roots_Node4_V7 (0)
16. Crown_Roots_Node5_V7 (0)
17. Crown_Roots_Node5_V13 (0)
18. Brace_Roots_Node6_V13 (0)
19. Coleoptile_GH_6DAS (7.0)
20. Pooled_Leaves_V1 (0)

21. Topmost_Leaf_V3 (0)
22. Shoot_Tip_V5 (0)
23. Tip_Stage2_Leaf_V5 (0)
24. Base_Stage2_Leaf_V5 (0)
25. Tip_Stage2_Leaf_V7 (8.1)
26. Base_Stage2_Leaf_V7 (0)
27. Eighth_Leaf_V9 (44.4)
28. Eleventh_Leaf_V9 (0)
29. Thirteenth_Leaf_V9 (0)
30. Immature_Leaves_V9 (0)

31. Thirteenth_Leaf_VT (0)
32. Thirteenth_Leaf_R2 (0)
33. Leaf_0DAP (0)
34. Leaf_6DAP (53.9)
35. Leaf_12DAP (3.3)
36. Leaf_18DAP (0)
37. Leaf_24DAP (23.7)
38. Leaf_30DAP (53.3)
39. Stem_and_SAM_V1 (3.1)
40. Stem_and_SAM_V3 (0)

41. First_Internode_V5 (0)
42. Fourth_Internode_V9 (0)
43. Internode_0DAP (17.8)
44. Internode_6DAP (2.5)
45. Internode_12DAP (9.7)
46. Internode_18DAP (0)
47. Internode_24DAP (0)
48. Internode_30DAP (4.8)
49. Immature_Tassel_V13 (0)
50. Meiotic_Tassel_V18 (1.0)

51. Anthers_R1 (0)
52. Immature_Cob_V18 (0)
53. Pre-pollination_Cob_R1 (0)
54. Silks_R1 (0)
55. Whole_Seed_2DAP (0)
56. Whole_Seed_4DAP (0)
57. Whole_Seed_6DAP (0)
58. Whole_Seed_8DAP (0)
59. Whole_Seed_10DAP (0)
60. Whole_Seed_12DAP (0)

61. Whole_Seed_14DAP (0)
62. Whole_Seed_16DAP (0)
63. Whole_Seed_18DAP (0)
64. Whole_Seed_20DAP (0)
65. Whole_Seed_22DAP (0)
66. Whole_Seed_24DAP (0)
67. Endosperm_12DAP (0)
68. Endosperm_14DAP (0)
69. Endosperm_16DAP (0)
70. Endosperm_18DAP (0)

71. Endosperm_20DAP (0)
72. Endosperm_22DAP (0)
73. Endosperm_24DAP (0)
74. Embryo_16DAP (0)
75. Embryo_18DAP (0)
76. Embryo_20DAP (0)
77. Embryo_22DAP (0)
78. Embryo_24DAP (0)
79. Pericarp_18DAP (21.7)

140

141

GRMZM2G151649

GRMZM2G151649

1. Primary_Root_3DAS (102.6)	11. Primary_Root_Z2_7DAS (38.9)	21. Topmost_Leaf_V3 (24.4)	31. Thirteenth_Leaf_VT (187.3)	41. First_Internode_V5 (74.8)
2. Root_MZ_and_EZ_3DAS (73.6)	12. Primary_Root_Z3_7DAS (32.1)	22. Shoot_Tip_V5 (46.5)	32. Thirteenth_Leaf_R2 (122.5)	42. Fourth_Internode_V9 (33.9)
3. Root_DZ_3DAS (135.0)	13. Primary_Root_Z4_7DAS (53.4)	23. Tip_Stage2_Leaf_V5 (43.8)	33. Leaf_0DAP (108.1)	43. Internode_0DAP (262.4)
4. Root_CP_3DAS (167.7)	14. Crown_Roots_Nodes1-3_V7 (29.0)	24. Base_Stage2_Leaf_V5 (36.6)	34. Leaf_6DAP (116.7)	44. Internode_6DAP (152.5)
5. Root_Stele_3DAS (40.0)	15. Crown_Roots_Node4_V7 (33.2)	25. Tip_Stage2_Leaf_V7 (51.3)	35. Leaf_12DAP (42.7)	45. Internode_12DAP (201.2)
6. Primary_Root_GH_6DAS (85.6)	16. Crown_Roots_Node5_V7 (70.9)	26. Base_Stage2_Leaf_V7 (33.8)	36. Leaf_18DAP (57.0)	46. Internode_18DAP (194.4)
7. Root_System_7DAS (59.8)	17. Crown_Roots_Node5_V13 (67.1)	27. Eighth_Leaf_V9 (255.3)	37. Leaf_24DAP (98.0)	47. Internode_24DAP (250.0)
8. Primary_Root_7DAS (58.1)	18. Brace_Roots_Node6_V13 (22.3)	28. Eleventh_Leaf_V9 (96.7)	38. Leaf_30DAP (74.3)	48. Internode_30DAP (190.4)
9. Seminal_Roots_7DAS (39.1)	19. Coleoptile_GH_6DAS (42.3)	29. Thirteenth_Leaf_V9 (80.9)	39. Stem_and_SAM_V1 (19.4)	49. Immature_Tassel_V13 (18.6)
10. Primary_Root_Z1_7DAS (71.0)	20. Pooled_Leaves_V1 (34.0)	30. Immature_Leaves_V9 (59.1)	40. Stem_and_SAM_V3 (20.6)	50. Meiotic_Tassel_V18 (65.5)
51. Anthers_R1 (81.4)	61. Whole_Seed_14DAP (49.9)	71. Endosperm_20DAP (60.3)		
52. Immature_Cob_V18 (20.0)	62. Whole_Seed_16DAP (28.3)	72. Endosperm_22DAP (47.3)		
53. Pre-pollination_Cob_R1 (73.6)	63. Whole_Seed_18DAP (64.9)	73. Endosperm_24DAP (68.7)		
54. Silks_R1 (98.2)	64. Whole_Seed_20DAP (58.3)	74. Embryo_16DAP (11.1)		
55. Whole_Seed_2DAP (89.7)	65. Whole_Seed_22DAP (42.7)	75. Embryo_18DAP (46.7)		
56. Whole_Seed_4DAP (105.6)	66. Whole_Seed_24DAP (46.4)	76. Embryo_20DAP (0)		
57. Whole_Seed_6DAP (105.4)	67. Endosperm_12DAP (25.5)	77. Embryo_22DAP (9.3)		
58. Whole_Seed_8DAP (98.7)	68. Endosperm_14DAP (36.6)	78. Embryo_24DAP (20.6)		
59. Whole_Seed_10DAP (65.8)	69. Endosperm_16DAP (59.2)	79. Pericarp_18DAP (184.2)		
60. Whole_Seed_12DAP (55.9)	70. Endosperm_18DAP (84.9)			

143

144

GRMZM2G057023

GRMZM2G057023

1. Primary_Root_3DAS (150.6)	11. Primary_Root_Z2_7DAS (146.7)	21. Topmost_Leaf_V3 (376.0)	31. Thirteenth_Leaf_VT (369.4)	41. First_Internode_V5 (170.1)
2. Root_MZ_and_EZ_3DAS (178.1)	12. Primary_Root_Z3_7DAS (128.9)	22. Shoot_Tip_V5 (136.4)	32. Thirteenth_Leaf_R2 (339.7)	42. Fourth_Internode_V9 (75.5)
3. Root_DZ_3DAS (115.6)	13. Primary_Root_Z4_7DAS (127.4)	23. Tip_Stage2_Leaf_V5 (1026.7)	33. Leaf_0DAP (390.8)	43. Internode_0DAP (148.5)
4. Root_CP_3DAS (167.3)	14. Crown_Roots_Nodes1-3_V7 (120.1)	24. Base_Stage2_Leaf_V5 (104.4)	34. Leaf_6DAP (237.9)	44. Internode_6DAP (166.9)
5. Root_Stele_3DAS (125.0)	15. Crown_Roots_Node4_V7 (128.9)	25. Tip_Stage2_Leaf_V7 (373.5)	35. Leaf_12DAP (457.7)	45. Internode_12DAP (191.3)
6. Primary_Root_GH_6DAS (115.4)	16. Crown_Roots_Node5_V7 (120.9)	26. Base_Stage2_Leaf_V7 (62.9)	36. Leaf_18DAP (344.3)	46. Internode_18DAP (190.4)
7. Root_System_7DAS (114.9)	17. Crown_Roots_Node5_V13 (143.2)	27. Eighth_Leaf_V9 (234.3)	37. Leaf_24DAP (781.7)	47. Internode_24DAP (236.6)
8. Primary_Root_7DAS (133.6)	18. Brace_Roots_Node6_V13 (140.1)	28. Eleventh_Leaf_V9 (75.6)	38. Leaf_30DAP (719.6)	48. Internode_30DAP (182.0)
9. Seminal_Roots_7DAS (86.9)	19. Coleoptile_GH_6DAS (132.4)	29. Thirteenth_Leaf_V9 (70.9)	39. Stem_and_SAM_V1 (120.7)	49. Immature_Tassel_V13 (86.8)
10. Primary_Root_Z1_7DAS (117.1)	20. Pooled_Leaves_V1 (389.9)	30. Immature_Leaves_V9 (62.1)	40. Stem_and_SAM_V3 (169.5)	50. Meiotic_Tassel_V18 (87.2)
51. Anthers_R1 (127.0)	61. Whole_Seed_14DAP (230.5)	71. Endosperm_20DAP (346.2)		
52. Immature_Cob_V18 (98.4)	62. Whole_Seed_16DAP (276.1)	72. Endosperm_22DAP (332.7)		
53. Pre-pollination_Cob_R1 (254.8)	63. Whole_Seed_18DAP (251.2)	73. Endosperm_24DAP (384.1)		
54. Silks_R1 (142.1)	64. Whole_Seed_20DAP (259.5)	74. Embryo_16DAP (214.3)		
55. Whole_Seed_2DAP (352.6)	65. Whole_Seed_22DAP (254.8)	75. Embryo_18DAP (229.4)		
56. Whole_Seed_4DAP (259.3)	66. Whole_Seed_24DAP (292.2)	76. Embryo_20DAP (198.6)		
57. Whole_Seed_6DAP (95.0)	67. Endosperm_12DAP (291.4)	77. Embryo_22DAP (176.4)		
58. Whole_Seed_8DAP (155.1)	68. Endosperm_14DAP (271.6)	78. Embryo_24DAP (139.0)		
59. Whole_Seed_10DAP (147.4)	69. Endosperm_16DAP (265.5)	79. Pericarp_18DAP (176.6)		
60. Whole_Seed_12DAP (167.5)	70. Endosperm_18DAP (287.3)			

146

25

147 **Supplementary Figure 7** The RNA-seq gene atlas for four genes (GRMZM2G180490, GRMZM2G010702, GRMZM2G151649 and

148 GRMZM2G057023) of maize inbred B73 includes 79 distinct replicated samples, these four figures from database of maizegdb (ULR:

149 http://www.maizegdb.org/gene_center/gene/).

150

Supplementary Figure 8 Experimental design. A total of 167 maize recombinant lines with 2 replications were screened every three days (total 16 time points). 100 diversity inbred lines with four replications were screened using RAP and manually measured. And the BLUP data of yield from the same 167 maize recombinant lines at 7 environments were used for yield predication.

157
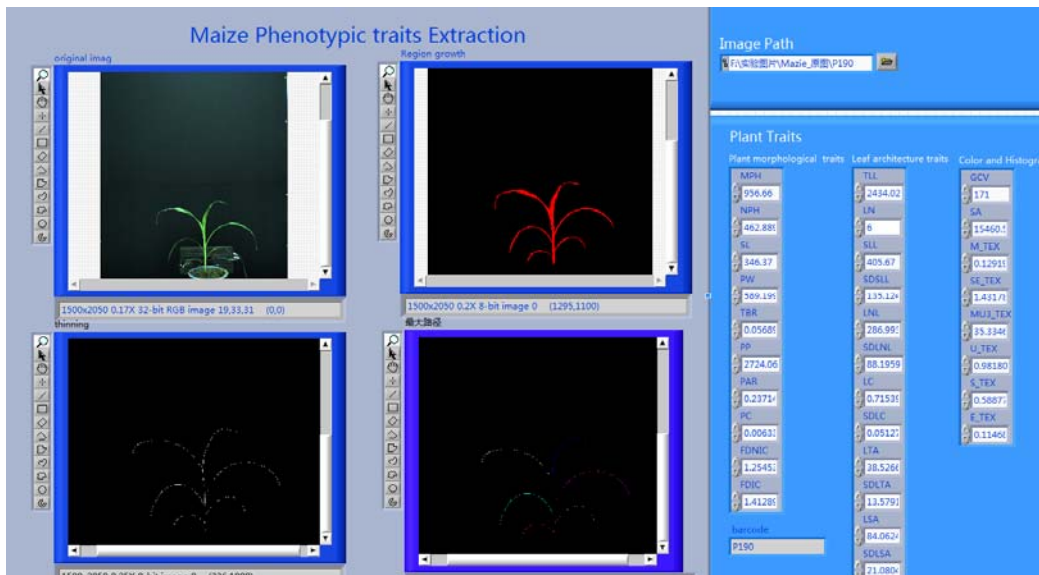
Supplementary Figure 9 The image analysis interface designed in the study.

161
162

163

164

165

28
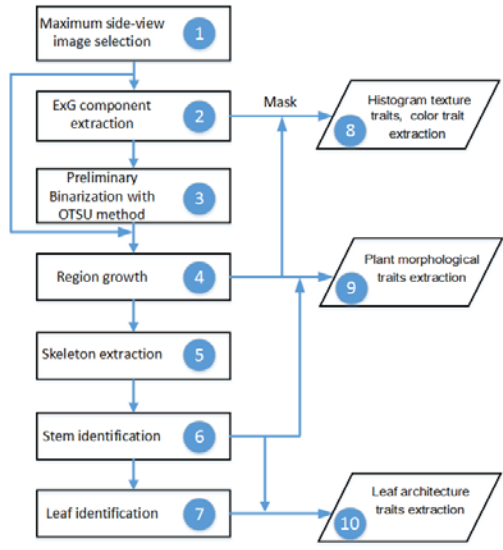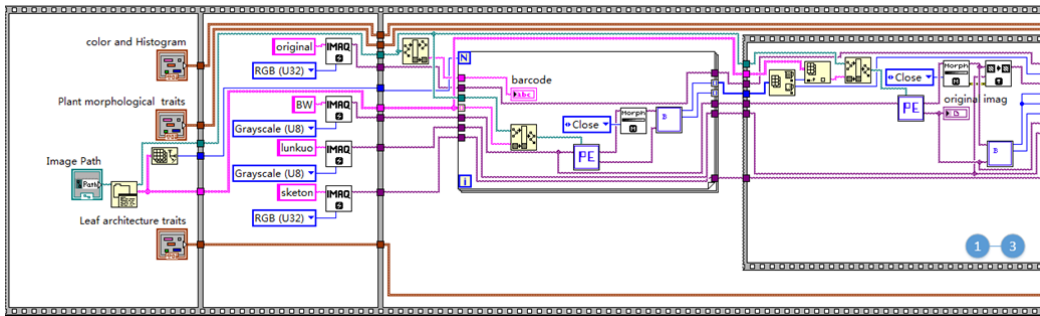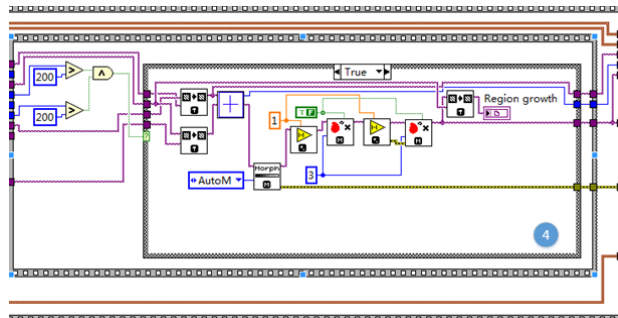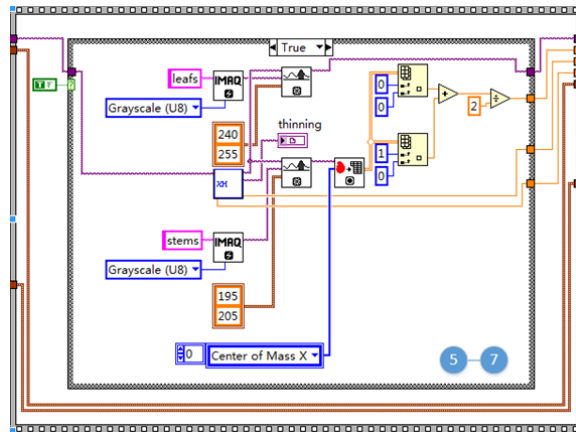
166
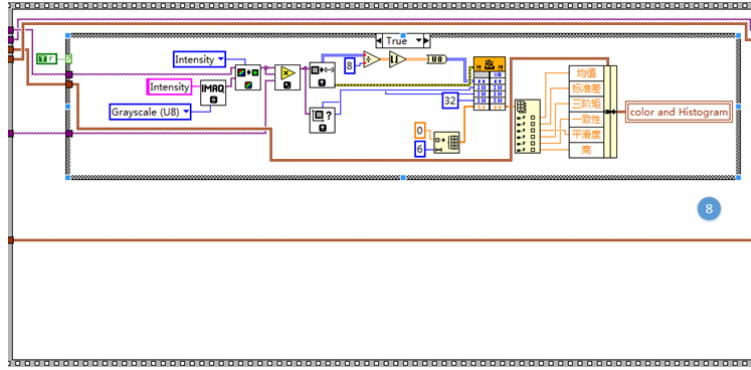
167
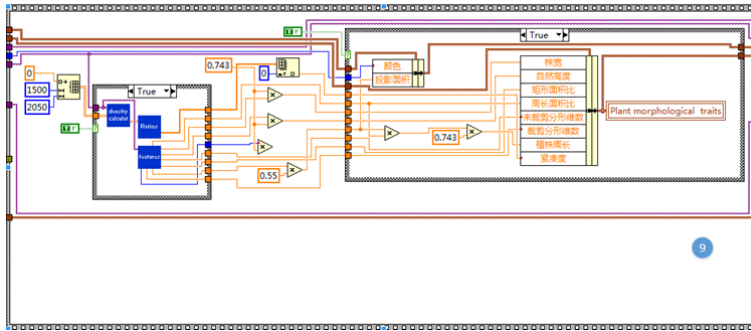
168
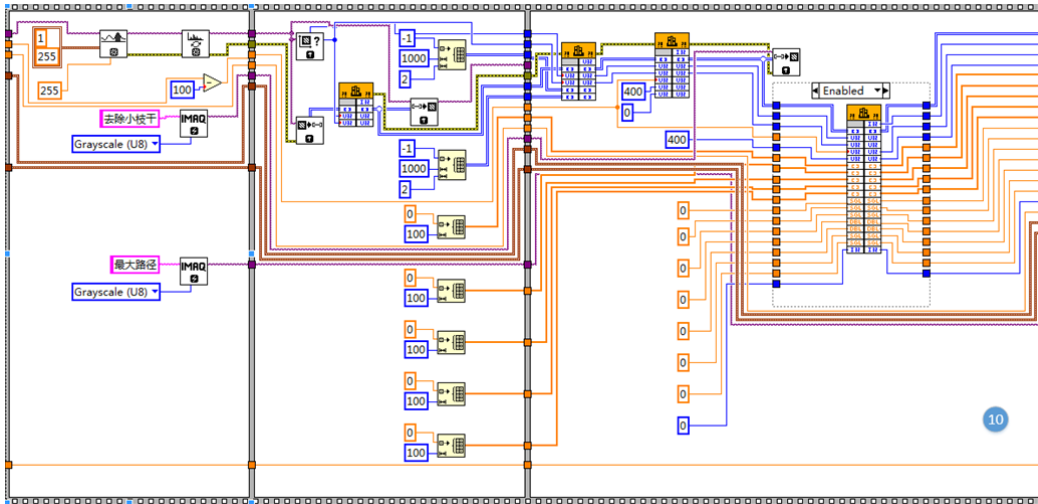
169
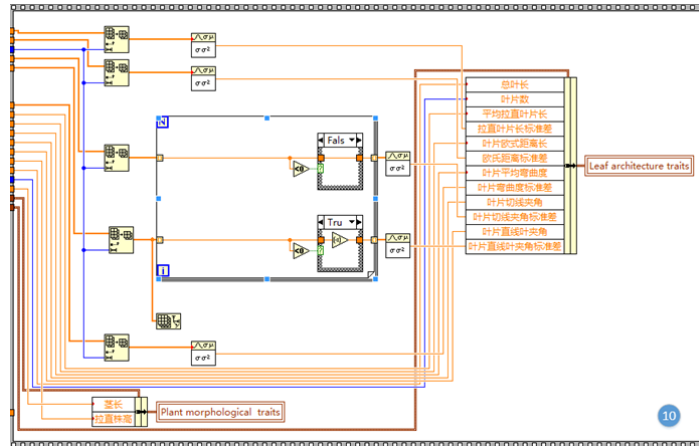
170   **Supplementary Figure 10** The flow chart of the program. The number represents

171   the processing module of the following figure 1~10.

172

173 **Supplementary Table 1** The 106 traits classification and abbreviation. More details

174 about the traits extraction can be found in the Supplementary Note 1.

Trait classification	Trait	Trait abbreviation	Trait definition
Plant morphological traits	Maximum plant height in side view	MPH	Seen in the Supplementary Note 1.
	Natural plant height in side view	NPH	
	Stem length in side view	SL	
	Plant width in side view	PW	
	Total projected area / bounding rectangle area ratio in side view	TBR	
	Plant perimeter in side view	PP	
	Perimeter / projected area ratio in side view	PAR	
	Plant compactness in side view	PC	
	Fractal dimension without image cropping in side view	FDNIC	
	Fractal dimension with image cropping in side view	FDIC	
Leaf architecture traits	Total leaf length per plant	TLL	
	Leaf number per plant	LN	
	Average straightened leaf length per plant	SLL	
	Standard deviation of straightened leaf length per plant	SDSLL	
	Average distance between the leaf tip and node per plant	LNL	
	Standard deviation of the distance between the leaf tip and node per plant	SDLNL	
	Average leaf curvature per plant	LC	
	Standard deviation of leaf curvature per plant	SDLC	
	Average leaf tangency angle per plant	LTA	
	Standard deviation of leaf tangency angle per plant	SDLTA	
	Average leaf straight angle per plant	LSA	
	Standard deviation of leaf straight angle per plant	SDLSA	

31

	Average straightened leaf length in lower half of plant	SLL_below
	Average distance between the leaf tip and node in lower half of plant	LNL_below
	Average leaf curvature in lower half of plant	LC_below
	Average of leaf tangency angle in lower half of plant	LTA_below
	Average of leaf straight angle in lower half of plant	LSA_below
	Average straightened leaf length in upper half of plant	SLL_above
	Average distance between the leaf tip and node in upper half of plant	LNL_above
	Average leaf curvature in upper half of plant	LC_above
	Average of leaf tangency angle in upper half of plant	LTA_above
	Average of leaf straight angle in upper half of plant	LSA_above
Color traits	Green color value in side view	GCV
Biomass related traits	Side projected area	SA
	Fresh weight	FW
	Dry weight	DW
Histogram texture traits	the mean value	M_TEX
	the standard error	SE_TEX
	the third moment	MU3_TEX
	the uniformity	U_TEX
	the smoothness	S_TEX
	the entropy	E_TEX
Growth related traits	Absolute growth rate	AGR_i (i=1,...,15)	Calculated using FW and
	Arithmetic mean value of the 15 absolute growth rates	MEAN_AGR	DW,

Relative growth rate	RGR_i	respectively
	$(i=1,...,15)$	
Arithmetic mean value of the 15 relative growth rates	MEAN_RGR	

175

176 **Supplementary Table 2** Statistical summary of the 10 developed models for fresh weight estimation (sample size = 387)*.

No.	Model classification	Model	coefficients	Std. Error	t	Sig.	Adjusted R^2	MAPE	SD_{APE}
1	Linear model	$FW = a_0 + a_1 \times SA_{max}$	a_0 = -6.539	1.211	-5.399	0.000	0.955	13.99%	13.34%
			a_1 = 6.23E-004	0.000	90.840	0.000			
2	Linear model	$FW = a_0 + a_1 \times SA_{ave}$	a_0 = -10.494	1.091	-9.620	0.000	0.965	14.28%	20.34%
			a_1 = 7.80E-004	0.000	103.916	0.000			
3	Linear model	$FW = a_0 + a_1 \times SA_1$	a_0 = -5.786	1.657	-3.492	0.001	0.918	21.28%	17.50%
			a_1 = 7.45E-004	0.000	65.525	0.000			
4	Linear model	$FW = a_0 + a_1 \times TA$	a_0 = 16.536	1.754	9.426	0.000	0.874	54.94%	75.07%
			a_1 = 2.74E-004	0.000	51.765	0.000			
5	Linear model	$FW = a_0 + a_1 \times SA_{max} + a_2 \times TA$	a_0 = -4.042	1.243	-3.253	0.001	0.959	14.98%	13.48%
			a_1 = 5.23E-004	0.000	28.121	0.000			
			a_2 = 4.9E-005	0.000	5.732	0.000			
6	Linear model	$FW = a_0 + a_1 \times (SA_{max} + SA_{min} + TA)$	a_0 = 3.807	1.313	2.901	0.004	0.940	28.16%	31.88%
			a_1 = 1.65E-004	0.000	77.469	0.000			
7	Quadratic model	$FW = a_0 + a_1 \times SA_{max} + a_2 \times SA_{max}^2$	a_0 = -12.909	1.651	-7.821	0.000	0.958	16.98%	26.05%
			a_1 = 7.41E-004	0.000	32.780	0.000			

34

			$a_2 = -3.22E-010$	0.000	-5.462	0.000			
8	Exponential	$FW = a_0 \times e^{a_1 \times SA_{max}}$	$a_0 = 13.176$	0.519	25.395	0.000	0.818	45.33%	54.14%
			$a_1 = 9.3E-006$	0.000	41.725	0.000			
9	Power model	$ln(FW) = a_0 + a_1 \times ln(SA_{max})$	$a_0 = -10.234$	0.103	-99.594	0.000	0.980	12.31%	9.97%
			$a_1 = 1.229$	0.009	137.697	0.000			
10	Power model	$ln(FW) = a_0 + a_1 \times ln(SA_{max}) + a_2 \times ln(TA)$	$a_0 = -10.081$	0.137	-73.693	0.000	0.980	12.34%	9.77%
			$a_1 = 1.147$	0.049	23.191	0.000			
			$a_2 = 0.067$	0.040	1.680	0.094			

177 *FW is fresh weight. SA_{max}, SA_{min}, SA_{ave}, SA_1 are the maximum projected area among 15 side view images, minimum projected area among 15

178 side view images, average projected area among 15 side view images, the first image among 15 side view images, respectively. TA is projected

179 area in top view.

180

Supplementary Table 3 Statistical summary of the 10 developed models for dry weight estimation (sample size = 387)*.

No.	Model classification	Model	coefficients	Std. Error	t	Sig.	Adjusted R^2	MAPE	SD_{APE}
1	Linear model	$DW = a_0 + a_1 \times SA_{max}$	$a_0 = -1.235$	0.163	-7.561	0.000	0.931	20.22%	29.99%
			$a_1 = 6.7E\text{-}005$	0.000	72.341	0.000			
2	Linear model	$DW = a_0 + a_1 \times SA_{ave}$	$a_0 = -1.175$	0.171	-9.321	0.000	0.928	24.89%	42.37%
			$a_1 = 8.1E\text{-}005$	0.000	70.737	0.000			
3	Linear model	$DW = a_0 + a_1 \times SA_1$	$a_0 = -1.109$	0.212	-5.220	0.000	0.886	22.06%	25.80%
			$a_1 = 8.0E\text{-}005$	0.000	54.655	0.000			
4	Linear model	$DW = a_0 + a_1 \times TA$	$a_0 = 1.158$	0.191	6.058	0.000	0.874	49.76%	70.17%
			$a_1 = 3.0E\text{-}005$	0.000	51.703	0.000			
5	Linear model	$DW = a_0 + a_1 \times SA_{max} + a_2 \times TA$	$a_0 = -0.816$	0.164	-4.988	0.000	0.940	16.87%	19.59%
			$a_1 = 5.0E\text{-}005$	0.000	20.480	0.000			
			$a_2 = 8.3E\text{-}006$	0.000	7.304	0.000			
6	Linear model	$DW = a_0 + a_1 \times (SA_{max} + SA_{min} + TA)$	$a_0 = -0.176$	0.156	-1.130	0.259	0.928	21.52%	21.97%
			$a_1 = 1.8E\text{-}005$	0.000	70.421	0.000			
7	Quadratic model	$DW = a_0 + a_1 \times SA_{max} + a_2 \times SA_{max}^2$	$a_0 = -0.781$	0.229	-3.411	0.001	0.933	16.59%	18.22%
			$a_1 = 5.9E\text{-}005$	0.000	18.667	0.000			

No.	Model	Equation	Parameter						
			$a_2 = 2.3E\text{-}011$	0.000	2.812	0.005			
8	Exponential model	$DW = a_0 \times e^{a_1 \times SA_{max}}$	$a_0 = 1.211$	0.049	24.564	0.000	0.820	48.15%	57.91%
			$a_1 = 9.7E\text{-}006$	0.000	41.960	0.000			
9	Power model	$ln(DW) = a_0 + a_1 \times ln(SA_{max})$	$a_0 = -13.047$	0.128	-101.593	0.000	0.971	15.85%	13.73%
			$a_1 = 1.270$	0.011	113.906	0.000			
10	Power model	$ln(DW) = a_0 + a_1 \times ln(SA_{max}) + a_2 \times ln(TA)$	$a_0 = -12.937$	0.171	-75.482	0.000	0.971	15.83%	13.73%
			$a_1 = 1.211$	0.062	19.551	0.000			
			$a_2 = 0.048$	0.050	0.966	0.335			

182   *DW is dry weight. SA_{max}, SA_{min}, SA_{ave}, SA_1 are the maximum projected area among 15 side view images, minimum projected area among 15

183   side view images, average projected area among 15 side view images, the single image with an angle of 0°, respectively. TA is projected area in

184   top view.

Supplementary Table 4 Summary of QTL for Growth Rate Related Trait Identified at Sixteen Time Points.

Trait	No. of Time Points[a]	No. of QTLs (Mean and Range)	PVE (%, Mean and Range)[b]	No. of QTLs
AGR_DW	8 (16)	1.5 (1-3)	10.0 (7.9-15.7)	12
RGR_DW	5 (16)	1.8 (1-3)	8.8 (7.5-10.0)	9
AGR_FW	9 (16)	1.8 (1-3)	10.0 (7.9-17.8)	16
RGR_FW	7 (16)	1.9 (1-4)	8.4 (7.3-10.2)	13

[a] Number of time points that have QTLs identified in this study; the total number of time points identified for each trait is in parentheses. [b]

Phenotypic variation explained (PVE) by each QTL.

190 **Supplementary Table 5** Statistical summary of the 6 developed models for digital biomass accumulation (167 samples × 16 time points).

Model	Model solution	Training set				Testing set			
		Number of time points	R^2	MAPE	SD_{APE}	Number of time points	R^2	MAPE	SD_{APE}
Linear model	$DB = b + a \times t$	5	0.975	6.2%	4.9%	11	0.716	47.3%	23.1%
		6	0.977	6.9%	6.3%	10	0.726	48.3%	21.1%
		7	0.973	8.2%	7.9%	9	0.707	49.7%	18.2%
		8	0.951	12.2%	11.5%	8	0.711	48.7%	15.7%
		9	0.938	16.5%	16.3%	7	0.699	47.9%	12.4%
		10	0.9	24.4%	25.8%	6	0.711	43.6%	10.9%
		11	0.889	32.6%	36.1%	5	0.709	39.7%	9.4%
Power model	$DB = at^b$	5	0.957	8.6%	7%	11	0.568	52.8%	23.6%
		6	0.964	9.2%	9.3%	10	0.63	51.4%	21.6%
		7	0.966	10.2%	11.4%	9	0.623	50.5%	18.6%
		8	0.958	13.4%	15.4%	8	0.665	45.4%	16%
		9	0.963	16.1%	19.2%	7	0.678	40.3%	12.8%

		10	0.959	22.6%	24.3%	6	0.758	27%	11.1%
		11	0.971	25.7%	27.4%	5	0.789	17.3%	9.8%
Exponential model	$DB = ae^{bt}$	5	0.989	3.5%	2.9%	11	0.767	22.7%	25.2%
		6	0.989	4%	3.4%	10	0.814	15.9%	16.2%
		7	0.989	4.8%	4.3%	9	0.788	16%	14.7%
		8	0.99	4.9%	4.3%	8	0.797	14.5%	14.4%
		9	0.993	4.9%	4.6%	7	0.803	14.6%	13.8%
		10	0.991	5.9%	4.7%	6	0.838	17.8%	19.2%
		11	0.994	5.8%	5%	5	0.834	20.3%	18.9%
Logarithm model	$DB = a\,ln(bt)$	5	0.893	13.5%	7.5%	11	0.314	63.5%	22.1%
		6	0.878	16.6%	11.2%	10	0.331	63.8%	20.2%
		7	0.856	20.4%	15.1%	9	0.336	64.6%	17.3%
		8	0.803	26.5%	21.9%	8	0.359	64.1%	15.1%
		9	0.766	33.5%	30.4%	7	0.381	63.6%	12%
		10	0.701	43.3%	45.2%	6	0.422	60.9%	10.5%

		11	0.672	55.4%	60.7%	5	0.467	58.1%	8.9%
Quadratic model	$DB = at^2 + bt + c$	5	0.992	2.7%	2.4%	11	0.753	25%	17.9%
		6	0.994	3%	2.7%	10	0.759	30%	18.1%
		7	0.994	3.4%	3%	9	0.709	33.1%	17.4%
		8	0.99	4.4%	3.6%	8	0.794	27%	13.9%
		9	0.991	5%	4.4%	7	0.811	24.7%	11.2%
		10	0.985	8.6%	7.6%	6	0.868	14.7%	8.8%
		11	0.988	10.2%	10.4%	5	0.861	10.8%	7.6%
Logistic model	$DB = \dfrac{y_m}{1+(\dfrac{y_m}{y(1)}-1)e^{-rt}}$	5	0.968	6.6%	6.4%	11	0	354.8%	6837.8%
		6	0.976	7.1%	6.2%	10	0.001	119.5%	552.6%
		7	0.98	7.9%	6.1%	9	0	160%	1732.4%
		8	0.973	10.6%	7.7%	8	0.006	218.1%	2381%
		9	0.98	11.2%	7.8%	7	0.001	369.4%	8291.9%
		10	0.978	14.5%	9.4%	6	0.002	208%	1836%
		11	0.983	14.2%	9.6%	5	0.568	23%	36.2%

191   *total 167 samples with 16 time points were used, and the dry weight values in 16 time points were divided into two parts: training set and

192   testing set. *DB* is the digital biomass; *t* is the time point; y_m is the saturation level of digital biomass; *y(1)* is the digital biomass at the first time

193   point; *r* is intrinsic growth rate; other variables are constants.

194

195

196 **Supplementary Table 6** Detecting the phenotypic traits (not include growth related
197 traits) significantly associated with yield (Tons per hectare) and calculating the
198 percentage of the phenotypic variance explanation (R^2).

The number of time points	No. of the time points	Sample size	The number of predictors	R^2
1	1	167	2	0.097
	2	167	2	0.054
	3	167	3	0.085
	4	167	0	0
	5	167	4	0.109
	6	167	0	0
	7	167	1	0.026
	8	167	2	0.063
	9	167	3	0.091
	10	167	0	0
	11	167	1	0.057
	12	167	1	0.031
	13	167	2	0.061
	14	167	3	0.100
	15	167	2	0.064
	16	167	1	0.045
2*	5, 14	167	4	0.140
	5, 13	167	4	0.137
	2, 10	167	3	0.090
	8, 16	167	2	0.084
	7, 15	167	3	0.092
	4, 12	167	1	0.031
	3, 11	167	1	0.057

	4, 12	167	1	0.031
	1, 8	167	2	0.108
	5, 9	167	3	0.090
4*	1, 8, 9, 14	167	7	0.259
	3, 7, 11, 15	167	1	0.060
	4, 8, 12, 16	167	2	0.084
	2, 6, 10, 14	167	7	0.236
	1, 5, 8, 12	167	5	0.197
	4, 9, 12, 16	167	9	0.293
	1, 5, 9, 13	167	6	0.250
	4, 8, 12, 16	167	2	0.084
	1, 8, 9, 15	167	7	0.255
	1, 8, 9, 16	167	8	0.296
16*	1~16	167	16	0.546

*The number of time points was 2: (1) first divided the traits in 1-16 time points into 2 parts: 1-8 time points, and 9-16 time points; (2) then randomly selected one time point from each part; (3) analyzing the phenotypic traits of 2 time points significantly associated with yield using linear stepwise regression.

*The number of time points was 4: (1) first divided the traits in 1-16 time points into 4 parts: 1-4, 5-8, 9-12, and 13-16 time points; (2) then randomly selected one time point from each part; (3) analyzing the phenotypic traits of 4 time points significantly associated with yield using linear stepwise regression.

*The number of time points was 16: (1) analyzing the phenotypic traits of whole 16 time points significantly associated with yield using linear stepwise regression; (2) when the selected traits number was 16, the phenotypic variance explanation (R^2) was 0.546.

211 **Supplementary Table 7** The statistical details of coefficients in selected model for yield (time points: 1, 8, 9, 16 in the Supplementary Table 6).

Variable	Unstandardized coefficients		Standardized coefficients	t	Sig.	Correlation coefficient
	Beta	Std. Error	Beta			
(Constant)	-5.958631315	1.545129291	-	-3.856396581	0.000170319	-
FDIC_1	4.074374336	0.871183001	0.325337978	4.676829473	6.44704E-06	0.26126088
LTA_above_1	0.015439375	0.00718035	0.146492247	2.150225976	0.033139983	0.13366803
GCV_8	0.011257982	0.003785316	0.205465432	2.974119177	0.003425104	0.11361801
SDLC_8	3.915590568	1.201529835	0.247415027	3.25883757	0.001384015	0.17101926
LTA_above_9	-0.027602628	0.008084923	-0.241236636	-3.414086825	0.000823206	-0.1517652
LTA_below_9	0.023143027	0.005221208	0.337257196	4.43250423	1.78875E-05	0.15576905
LNL_above_16	0.000992047	0.000439417	0.157834234	2.257643508	0.025411289	0.19162319
LSA_below_16	-0.007914713	0.002375563	-0.251159956	-3.331721454	0.001086861	-0.0498452

212

213

214 **Supplementary Table 8** Candidate genes and their annotations located in the first three peak bins in QTL hot spot located on chromosome 10.

Bin	LOD	Candidate gene	Gene_start (bp)	Gene_end (bp)	Gene_lengh (bp)	Annotation
	7.338	GRMZM5G807276	90929578	90933166	3588	Flavonol synthase-like protein
	7.338	GRMZM2G089721	91086013	91087416	1403	C2H2 zinc finger protein
	7.338	GRMZM2G306237	91132646	91134810	2164	unknown
	7.338	GRMZM2G039381	91170189	91171172	983	plantacyanin
	7.338	GRMZM2G329559	91356652	91359020	2368	unknown
Left bin	7.338	GRMZM2G038846	91359222	91360805	1583	Pathogenesis-related thaumatin superfamily protein
(51.11-51.41	7.338	GRMZM2G042164	91480073	91501698	21625	serine-type peptidase activity
cM or	7.338	GRMZM2G424651	91585407	91595431	10024	unknown
90.93-91.96	7.338	GRMZM2G140448	91679345	91681251	1906	electron carrier activity
Mb)	7.338	GRMZM2G116626	91713408	91720273	6865	galactosylceramidase activity
	7.338	GRMZM2G116704	91729914	91730391	477	unknown
	7.338	AC188000.3_FG003	91778426	91779253	827	unknown
	7.338	GRMZM2G347623	91780983	91788482	7499	unknown
	7.338	GRMZM2G419826	91858268	91858624	356	unknown
	7.338	GRMZM2G158141	91956237	91959657	3420	unknown
Peak bin	9.761	GRMZM2G176998	92132744	92135362	2618	unknown
(51.41-51.71	9.761	GRMZM2G582586	92305272	92305758	486	unknown
cM or	9.761	GRMZM2G110567	92536953	92538977	2024	unknown
91.96-94.97	9.761	GRMZM5G871827	92543634	92544361	727	unknown
Mb)	9.761	GRMZM2G549348	92543634	92544237	603	unknown
	9.761	GRMZM2G149698	92780255	92795025	14770	zinc ion binding

9.761	GRMZM2G025939	92823290	92831359	8069	sodium:dicarboxylate symporter activity
9.761	GRMZM2G174699	92909267	92914756	5489	hydrolase activity
9.761	GRMZM2G343291	93139717	93141352	1635	unknown
9.761	AC199571.3_FG004	93222605	93224374	1769	cell redox homeostasis
9.761	AC199571.3_FG003	93224472	93226100	1628	unknown
9.761	AC199571.3_FG001	93228585	93232585	4000	unknown
9.761	GRMZM2G450512	93377121	93377751	630	unknown
9.761	GRMZM2G061879	93396308	93397659	1351	cysteine-type endopeptidase activity
9.761	GRMZM2G018099	93439404	93439793	389	unknown
9.761	GRMZM2G048697	93634149	93634637	488	unknown
9.761	GRMZM5G833699	93684085	93687059	2974	ATP binding
9.761	GRMZM2G701389	93823514	93824012	498	unknown
9.761	GRMZM5G863097	93909832	93913928	4096	cation transmembrane transporter activity
9.761	GRMZM5G831308	93917114	93918884	1770	hydrolase activity
9.761	GRMZM5G818631	93924872	93926095	1223	unknown
9.761	GRMZM2G066044	94000687	94003652	2965	DNA binding
9.761	GRMZM2G701394	94035799	94036372	573	unknown
9.761	GRMZM2G006871	94053195	94054568	1373	unknown
9.761	GRMZM2G166899	94069900	94071281	1381	cofactor binding
9.761	GRMZM2G174773	94088449	94092547	4098	cation transmembrane transporter activity
9.761	GRMZM2G174671	94095402	94103354	7952	hydrolase activityn
9.761	GRMZM2G381691	94248710	94251264	2554	unknown
9.761	GRMZM2G077951	94589221	94591581	2360	unknown
9.761	GRMZM2G176737	94700361	94702957	2596	unknown
9.761	GRMZM2G079944	94725452	94728221	2769	shikimate kinase activity

	9.761	GRMZM2G034807	94878301	94879200	899	unknown
	9.761	GRMZM2G011928	94898386	94900563	2177	unknown
	9.761	AC208625.3_FG004	94943457	94944123	666	unknown
	9.761	GRMZM2G142680	94965435	94969104	3669	ATP binding
Right bin	5.915	GRMZM2G171716	95041622	95043310	1688	unknown
(51.71-52.31	5.915	GRMZM2G401883	95076585	95077348	763	unknown
cM or						
94.97-95.21	5.915	GRMZM2G131611	95122698	95125994	3296	unknown
Mb)						

215

Supplementary Table 9 Candidate genes and their annotations located in the first three peak bins in QTL hot spot located on chromosome 7.

Bin	LOD	Candidate gene	Gene_start (bp)	Gene_end (bp)	Gene_lengh (bp)	Annotation
	5.030	GRMZM2G066197	161619112	161620899	1787	adhesive/proline-rich protein
	5.030	GRMZM5G813007	161658285	161664104	5819	N-acetyl-gamma-glutamyl-phosphate reductase
	5.030	GRMZM2G396402	161684511	161685803	1292	unknown
	5.030	GRMZM2G396397	161685025	161693219	8194	NADH dehydrogenase (ubiquinone)
Left bin (161.42-161.95 Mb or 119.4-120.5 cM)	5.030	GRMZM2G096454	161695256	161696299	1043	unknown
	5.030	GRMZM5G898305	161696905	161700933	4028	unknown
	5.030	GRMZM2G096395	161703912	161705328	1416	unknown
	5.030	GRMZM5G893619	161704869	161705514	645	unknown
	5.030	GRMZM5G888034	161793838	161794406	568	unknown
	5.030	GRMZM2G179779	161801567	161802786	1219	unknown
	5.030	GRMZM2G179777	161804206	161805610	1404	triacylglycerol lipase
	5.030	GRMZM2G479163	161813482	161823445	9963	aminophospholipid ATPase 2
	5.030	GRMZM2G411916	161834088	161851386	17298	aminophospholipid ATPase 2
	5.030	GRMZM2G411940	161854577	161863059	8482	aminophospholipid ATPase 2
	5.030	GRMZM2G172657	161902122	161904577	2455	GRAS family transcription factor

	5.030	GRMZM2G172726	161919240	161923252	4012	unknown
	5.030	AC192356.3_FG003	161939954	161944649	4695	unknown
Peak bin (161.95-162.04 Mb or 120.5-121.4 cM)	5.192	GRMZM2G180490	161948926	161953678	4752	adenylyl-sulfate kinase
	5.192	GRMZM2G010702	161958265	161959052	787	unknown
	5.192	GRMZM2G151649	162003495	162005287	1792	ARM repeat superfamily protein
	5.192	GRMZM2G057023	162036068	162042246	6178	Interferon-related developmental regulator
Right bin (162.04-162.16 Mb or 121.4-122 cM)	5.026	GRMZM2G057176	162044113	162046668	2555	Pentatricopeptide repeat (PPR) superfamily protein
	5.026	GRMZM2G357734	162054794	162062790	7996	Serine C-palmitoyltransferase
	5.026	GRMZM2G057247	162068683	162075079	6396	actin binding
	5.026	GRMZM2G057260	162079660	162085372	5712	MOS4-associated complex 3B
	5.026	AC187046.3_FG009	162096143	162097954	1811	zinc knuckle family protein
	5.026	GRMZM2G089557	162149448	162150576	1128	zinc finger, C2H2 type family protein
	5.026	GRMZM2G089630	162153422	162157104	3682	integral membrane protein like

217

218 **Supplementary Table 10.** Comparison of published work for combination of high-throughput phenotyping and QTL/GWAS analysis.

Species	Population type	Population size	Marker	Identified loci/QTL	Platform, sensors or software	Traits	Application	Throughput	Measuring efficiency	Reference [*]
Arabidopsis and maize	Col-0 and C24; Three panels of diverse maize inbred lines	Arabidopsis: 2; Maize: 44, 25 and 63;	NA	NA	Visible, near-infrared, and fluorescence imaging (LemnaTec 3D Scanalyzer in IPK, Germany)	projected leaf area (Arabidopsis) and estimated volume(maize)	Indoor phenotyping for Arabidopsis and maize	384, 2304 or 4608 plants, up to 4600 Arabidopsis	30 second per plant	Junker et al., 2014
Maize	Association population	252	50k SNPs	12 loci	Visible light imaging (LemnaTec 3D Scanalyzer in IPK, Germany)	Shoot biomass, biomass accumulation	In door shoot biomass and growth	384, 2304 or 4608 plants, up to 4600 Arabidopsis	30 second per plant	Muraya et al., 2016
Wild Barley	Introgression lines	47	1,536-SNP barley BOPA1 set	44 QTL	Visible light imaging (LemnaTec 3D Scanalyzer in The Plant Accelerator)	14 biomass and plant growth related traits	Indoor phenotyping for drought tolerance	2400	30 second per plant	Honsdorf et al., 2014
Wheat	RIL population	150	3.2k SNPs	20 QTL	Visible light imaging (LemnaTec 3D Scanalyzer in The Plant Accelerator)	Biomass, plant weight, leaf area, average growth rate, and WUE	In door shoot phenotyping	2400	30 second per plant	Parent et al., 2015
Rice	RIL population	171	164 SSRs and RFLP	89 QTL	3D visible light imaging, GiA Roots, Rootwork software	25 Root system architecture traits	Root phenotyping of growth in a gellan gum	NA	NA	Topp et al., 2013

51

							medium			
Rice	Association population	242	700k SNPs	709 and 496 significant associations using two different methods.	PANorama	49 panicle phenotypes	Rice panicle architecture	NA	NA	Crowell et al., 2016
Arabidopsis	Association population	324	~215k SNPs	26 SNPs	PHENOPSIS phenotyping platform, top-view imaging	Fresh weight, Projected leaf area, growth related traits	Arabidopsis leaf phenotyping	540 pots	NA	Bac-Molenaar et al., 2015
Rice	Association population	167	one marker per 22.5 kb	51 loci	Rhizoscope phenotyping platform, Visible light imaging	15 shoot and root traits	Root phenotyping of growth in hydroponic system	192 plants	NA	Courtois et al., 2013
Rice	Association population	three panels: 455, 469, 389 accessions	4,358k, 2,863k, 1,959k SNPs for each panel	382 loci	High-throughput leaf scorer (HLS), linear scanning	29 leaf traits related to leaf size, shape, and color	Fast leaf phenotyping after clipping	NA	30 leaves per minute	Yang et al., 2015
Triticale	doubled haploid lines	647	1710 DArT markers	2 QTL	Breed Vision, 3D-Time-of-Flight camera; laser distance sensor; hyperspectral	Biomass accumulation	Field phenotyping in plot level	NA	more than 2,000 plots per day	Busemeyer et al., 2013

					imaging; light curtain imaging					
Pepper	RIL population	151	493 markers	10 QTL	RGB camera and distance camera	Leaf size, leaf angle, plant height, and total leaf area	Indoor phenotyping for tall plant	192 plants	3 min each single row	Van et al., 2012
Rice	Association population	533	4,358 k SNPs	141 QTL	Visible light imaging, x-ray CT, and linear scanning (HRPF, China)	6 shoot traits and 9 yield traits	In door shoot phenotyping and yield traits	5472 pots	45 second per plant	Yang et al., 2014
Maize	RIL population	167	2496 recombinant bins	988 QTL	Visible light imaging (HRPF, China)	106 traits: 10 plant morphological traits, 22 leaf architecture traits, 1 plant color trait, 3 biomass related traits, 6 histogram texture traits, and 64 growth related traits	In door shoot phenotyping	5472 pots	The time costs of plant screening and image analysis for each plant were 45s and 10	The present work in this article

219   *The references were listed at the end of supplementary information.

220   **Supplementary Table 11 Experimental schedule of maize plant phenotyping.**

Experimental design	Time point	Date of replicate 1	Date of replicate 2	Days after sowing	Sample size	Note
Sowing	Sowing date	2015.3.20	2015.3.21	-	721	2 replicates (334 maize plant) for non-destructive measurements and 387 maize plant for destructive measurements
Non-destructively measuring of maize plant	Time point 1	2015.4.11	2015.4.12	22	167	Screening of the maize plant and extracting the phenotypic traits
	Time point 2	2015.4.14	2015.4.15	25	167	
	Time point 3	2015.4.17	2015.4.18	28	167	
	Time point 4	2015.4.20	2015.4.21	31	167	
	Time point 5	2015.4.23	2015.4.24	34	167	
	Time point 6	2015.4.26	2015.4.27	37	167	
	Time point 7	2015.4.29	2015.4.30	40	167	
	Time point 8	2015.5.2	2015.5.3	43	167	
	Time point 9	2015.5.5	2015.5.6	46	167	
	Time point 10	2015.5.8	2015.5.9	49	167	
	Time point 11	2015.5.11	2015.5.12	52	167	
	Time point 12	2015.5.14	2015.5.15	55	167	
	Time point 13	2015.5.17	2015.5.18	58	167	
	Time point 14	2015.5.20	2015.5.21	61	167	
	Time point 15	2015.5.23	2015.5.24	64	167	
	Time point 16	2015.5.26	2015.5.27	67	167	

Manually measuring of maize plant	-	Measuring date	-	Days after sowing	Sample size	Note
	1	2015.4.25	-	36	103	Measuring the
	2	2015.5.7	-	48	101	maize plant
	3	2015.5.19	-	60	99	height, fresh
	4	2015.5.29	-	70	84	weight, and dry
	Total				387	weight

221 **Supplementary Table 12 The detailed information of Sub-vi and Dynamic link**

222 **library (DLL) used in the study.** Source code can be downloaded using the link:

223 http://plantphenomics.hzau.edu.cn/checkiflogin_en.action (Username: UserPP,

224 Password: 20170108pp)

VI and DLL list	Function Explanation	Supplement
Processing.vi	Gray image extraction and preliminary segmentation.	
Index.vi	Calculating the plant width with the binary image, in order to select the maximum side-view image.	
RegionGrow.vi	To complete the whole plant image with the preliminary binary image and neighborhood information	
DensityCalculation.vi	To calculate the image density	
RatioCalculation.vi	To obtain the plant compactness with the density information.	
FeaturesCalculation.vi	To calculate the plant morphological traits.	
SkeletonExtraction.vi	To extract the skeleton and identify the maize leaf	
Nebogrow.dll	To complete the maize image.	int Nebogrow (unsigned int *pImag, // Original color image unsigned char *Graybuff, // Preliminary binary image unsigned int BWWidth, // Image width unsigned int BWHeight) // Image height
Thinning.dll	To extract the skeleton of maize image	int Thinning(unsigned char *Array, //binary image unsigned int width, //Image width

56

		unsigned int height) // Image height
FreeEndDectet.dll	To identify the endpoints and nodes	int FreeEndDetect(unsigned char *Array, //Skeleton image unsigned int BWWidth,// Image width unsigned int BWHeight, // Image height int *EndArray, // Endpoints int *JunctionArray) //Nodes
SkeletonFollow.dll	To mark each leaf and stem.	int SkeletonFollow(unsigned char *p, //Skeleton image unsigned int _BWWidth, // Image width unsigned int _BWHeight) // Image height
PathExtra.dll	To identify the maize leaf and stem	int pathExtra_forleaf (unsigned char *Array,// Skeleton image unsigned int _BWWidth,// Image width unsigned int _BWHeight,// Image height)
PathForSingle.dll	To calculate the leaf architecture traits	İnt PathExtra_Single(unsigned char *Array, // skeleton image unsigned int _BWWidth, //image width unsigned int _BWHeight, //image height unsigned int _Xstart, //start position unsigned int _Distance, //searching distance float *leaflength, //each leaf length float *OClength, //each leaf euclidean distance double *angle, //each leaf tangency angle double *angle1, //each leaf straight angle float *WanQD, //each leaf curvature

		float &Mean_length, //SLL; float &Mean_OClength, //LNL float &Mean_WanQD,//LC double &Mean_Angle, //LTA double &Mean_Angle1,//LSA float &lazhizhugao, //MPH float &total_leaflength, //TLL int &leaf_number //LN)//parameters calculation
binarization.dll	To obtain the preliminary binary image.	void TOPim2bw2(uint8_t *R, uint8_t *G, uint8_t *B, int32_t row, int32_t col, float EGthreshold, float ERthreshold, uint8_t *bw);
fractaldim.dll	To calculate the fractal dim of the plant.	void box_counting(uint8_t *bw, int32_t row, int32_t col, int32_t area, float *FD);
HistProperty.dll	To calculate the texture features of maize plant.	uint8_t HistProperty(uint8_t *Im, int32_t row, int32_t col, int32_t G, double *HistStat);
PlantType.dll	To calculate the plant compactness feature.	void CalLeafDens(uint8_t *bw, int32_t row, int32_t col, int32_t GridSize, float *dens); void DensClassify(float *dens, int32_t row, int32_t col, float *ratio);
imFillRemove.dll	To remove the small area noise.	void bwremove(uint8_t *bw, int32_t row, int32_t col, int32_t areathreshold);

225

226

227

228

Supplementary Note 1. Definition of the features

● Maximum plant height in side view (MPH): With the skeleton image (Supplementary Figure 1f), the leaf length and the distance from the leaf base point to stem base point (aboveground) was calculated for each leaf; and the maximum summation was selected as the maximum plant height.

● Natural plant height in side view (NPH): With the whole binary image (Supplementary Figure 1c), the vertical distance from plant tip to stem base (aboveground) was computed as the natural plant height.

● Stem length in side view (SL): With the stem identified image (Supplementary Figure 1e), the red line was identified as the stem and the length of the red was regarded as stem length.

● Plant width in side view (PW): As shown in the whole binary image (Supplementary Figure 1c), the horizontal distance from the left first foreground pixel to the right last foreground pixel was acquired as the plant width.

● Total projected area / bounding rectangle area ratio in side view (TBR): With the whole binary image (Supplementary Figure 1c), the TBR was calculated by the ratio of total projected area to the bounding rectangle area.

● Plant perimeter in side view (PP): With the whole binary image (Supplementary Figure 1c), the contour of the plant area was extracted and the PP was calculated as the summation of the foreground pixels.

● Plant compactness in side view (PC): Divide the image into several sub-images using a (5 × 5) window. And calculate the ratio of the foreground pixels to the total number of pixels in each sub-image (5 × 5), denoted as plant compactness in each sub-image (PCs). Then Count the number of PCs belonging to the class: 80-100%, denoted as ND. At last, leaf compactness (PC) was computed as the percentage of ND compared to the total PCs number.

● Fractal dimension with/without image cropping in side view: Superimpose boxes with box size of δ_k on the interested object, and calculate the number of boxes that are needed to cover the object, denoted as N_{δ_k}. Repeat this process with reducing δ_k

258 until δ_k approaches pixel size. Fractal dimension was calculated using the following

259 Equation. The fractal dimension for the image cropped by the minimum bounding

260 rectangle was calculated as the fractal dimension with image cropping (FDIC). On the

261 contrary, the fractal dimension for non-cropping image was computed as the fractal

262 dimension without image cropping (FDNIC).

263 $$FD = \lim_{\delta_k \to 0} \frac{\ln N_{\delta_k}}{-\ln \delta_k} \qquad (1)$$

264 ● Total leaf length per plant (TLL): With the skeleton image (Supplementary Figure

265 1f), each leaf was identified and the leaf length was calculated. The TLL is the

266 summation of all the leaf length.

267 ● Leaf number per plant (LN): As shown in the skeleton image (Supplementary

268 Figure 1f), each leaf was identified and labeled with different color. The color number

269 indicated the leaf number per plant.

270 ● Average straightened leaf length per plant (SLL): As shown in the skeleton image

271 (Supplementary Figure 1f), the leaf length was extracted as the straightened distance

272 from leaf tip to leaf base, and then SLL was calculated by the average value of all the

273 leaf length.

274 ● Average distance between the leaf tip and node per plant (LNL): As shown in the

275 skeleton image (Supplementary Figure 1f), the leaf distance was extracted as the

276 natural distance from leaf tip to leaf base, and then LNL was calculated by the

277 average value of all the leaf distance.

278 ● Average leaf curvature per plant (LC): As shown in the skeleton image

279 (Supplementary Figure 1f), the leaf curvature was computed by the ratio of leaf

280 distance to leaf length, and then LC was calculated as the average value of all the leaf

281 curvature.

282 ● Average leaf tangency angle per plant (LTA): As shown in the skeleton image

283 (Supplementary Figure 1f), leaf tangency angle was defined as the angle of leaf base

284 tangent line and stem line, and then LTA was calculated as the average value of all the

285 leaf tangency angle.

286 ● Average leaf straight angle per plant (LSA): As shown in the skeleton image

(Supplementary Figure 1f), leaf straight angle was defined as the angle of the leaf distance line and stem line, and then LSA was calculated as the average value of all the leaf straight angle.

● Average straightened leaf length in lower half of plant (SLL_below) and average straightened leaf length in upper half of plant (SLL_above): From the top leaf to the bottom leaf, SLL of all the leaves were averagely divided to 2 parts: upper half part and below half part. The average of SLL in below half part was identified as SLL_below, and the average of SLL in upper half part was identified as SLL_above.

● Average distance between the leaf tip and node in lower half of plant (LNL_below) and average distance between the leaf tip and node in upper half of plant (LNL_above): From the top leaf to the bottom leaf, LNL of all the leaves were averagely divided to 2 parts: upper half part and below half part. The average of LNL in below half part was identified as LNL_below, and the average of LNL in upper half part was identified as LNL_above.

● Average leaf curvature in lower half of plant (LC_below) and average leaf curvature in upper half of plant (LC_above): From the top leaf to the bottom leaf, LC of all the leaves were averagely divided to 2 parts: upper half part and below half part. The average of LC in below half part was identified as LC_below, and the average of LC in upper half part was identified as LC_above.

● Average of leaf tangency angle in lower half of plant (LTA_below) and average of leaf tangency angle in upper half of plant (LTA_above): From the top leaf to the bottom leaf, LTA of all the leaves were averagely divided to 2 parts: upper half part and below half part. The average of LTA in below half part was identified as LTA_below, and the average of LTA in upper half part was identified as TLA_above.

● Average of leaf straight angle in lower half of plant (LSA_below) and average of leaf straight angle in upper half of plant (LSA_above): From the top leaf to the bottom leaf, LSA of all the leaves were averagely divided to 2 parts: upper half part and below half part. The average of LSA in below half part was identified as LSA_below, and the average of LSA in upper half part was identified as LSA_above.

● Green color value (GCA): the ExG value was computed for each foreground

317   pixel in the grayscale image and the average value was calculated as the green color

318   value.

319   ●   Side Projected area (SA): Number of foreground pixels in the side-view image.

320   ●   The 6 histogram features, including the mean value (M_TEX), the standard error

321   (SE_TEX), the third moment (MU3_TEX), the uniformity (U_TEX), the smoothness

322   (S_TEX) and the entropy (E_TEX), were calculated using the following equations.

323

$$M = \sum_{i=0}^{L-1} G_i p(G_i)$$

(2)

324

$$SE = \sqrt{\sum_{i=0}^{L-1} (G_i - M)^2 p(G_i)}$$

(3)

325

$$MU3 = \sum_{i=0}^{L-1} (G_i - M)^3 p(G_i)$$

(4)

326

$$U = \sum_{i=0}^{L-1} p^2(G_i)$$

(5)

327

$$S = 1 - \frac{1}{1 + SE^2}$$

(6)

328   ●   Absolute growth rate (AGR$_i$): the absolute growth rate was calculated using the

329   following equation:

330

$$AGR_i = Biomass_{i+1} - Biomass_i \quad (i=1,...,15)$$

(7)

331   Where Biomass was fresh weight or dry weight at *ith* time points.

332   ●   Relative growth rate (RGR$_i$): the relative growth rate was calculated using the

333   following equation:

334

$$RGR_i = \frac{Biomass_{i+1} - Biomass_i}{Biomass_i} \quad (i=1,...,15)$$

(8)

335   Where Biomass$_i$ was fresh weight or dry weight at *ith* time points.

336

337

338

References

The references mentioned in the Supplementary Table 10 were listed as follows:

Bac-Molenaar JA, Vreugdenhil D, Granier C, Keurentjes JJ (2015) Genome-wide association mapping of growth dynamics detects time-specific and general quantitative trait loci. J Exp Bot **66:** 5567-5580

Busemeyer L, Ruckelshausen A, Moller K, Melchinger AE, Alheit KV, Maurer HP, Hahn V, Weissmann EA, Reif JC, Wurschum T (2013) Precision phenotyping of biomass accumulation in triticale reveals temporal genetic patterns of regulation. Sci Rep **3:** 2442

Courtois B, Audebert A, Dardou A, Roques S, Ghneim-Herrera T, Droc G, Frouin J, Rouan L, Goze E, Kilian A, Ahmadi N, Dingkuhn M (2013) Genome-wide association mapping of root traits in a japonica rice panel. PLoS One **8:** e78037

Crowell S, Korniliev P, Falcao A, Ismail A, Gregorio G, Mezey J, McCouch S (2016) Genome-wide association and high-resolution phenotyping link Oryza sativa panicle traits to numerous trait-specific QTL clusters. Nat Commun **7:** 10527

Honsdorf N, March TJ, Berger B, Tester M, Pillen K (2014) High-throughput phenotyping to detect drought tolerance QTL in wild barley introgression lines. PLoS One **9:** e97047

Junker A, Muraya MM, Weigelt-Fischer K, Arana-Ceballos F, Klukas C, Melchinger AE, Meyer RC, Riewe D, Altmann T (2014) Optimizing experimental procedures for quantitative evaluation of crop plant performance in high throughput phenotyping systems. Front Plant Sci **5:** 770

Muraya MM, Chu J, Zhao Y, Junker A, Klukas C, Reif JC, Altmann T (2016) Genetic variation of growth dynamics in maize (Zea mays L.) revealed through automated non-invasive phenotyping. Plant J

Parent B, Shahinnia F, Maphosa L, Berger B, Rabie H, Chalmers K, Kovalchuk A, Langridge P, Fleury D (2015) Combining field performance with controlled environment plant imaging to identify the genetic control of growth and transpiration underlying yield response to water-deficit stress in wheat. J Exp Bot **66:** 5481-5492

Topp CN, Iyer-Pascuzzi AS, Anderson JT, Lee CR, Zurek PR, Symonova O, Zheng Y, Bucksch A, Mileyko Y, Galkovskyi T, Moore BT, Harer J, Edelsbrunner H, Mitchell-Olds T, Weitz JS, Benfey PN (2013) 3D phenotyping and quantitative trait locus mapping identify core regions of the rice genome controlling root architecture. Proc Natl Acad Sci U S A **110:** E1695-1704

Van dHG, Song Y, Horgan G, Polder G, Dieleman A, Bink M, Palloix A, Van EF, Glasbey C (2012) SPICY: towards automated phenotyping of large pepper plants in the greenhouse. Funct Plant Biol **39:** 870-877

Yang W, Guo Z, Huang C, Duan L, Chen G, Jiang N, Fang W, Feng H, Xie W, Lian X, Wang G, Luo Q, Zhang Q, Liu Q, Xiong L (2014) Combining

high-throughput phenotyping and genome-wide association studies to reveal natural genetic variation in rice. Nat Commun **5:** 5087

Yang W, Guo Z, Huang C, Wang K, Jiang N, Feng H, Chen G, Liu Q, Xiong L (2015) Genome-wide association study of rice (Oryza sativa L.) leaf traits with a high-throughput leaf scorer. J Exp Bot **66:** 5605-561